https://doi.org/10.57634/RCR5076

Nanocellulose and its polymer composites: preparation, characterization, and applications

Ahmed Abdel-Hakim,[a]* Reda Mourad [b]

[a] *Materials Testing and Surface Chemical Analysis Laboratory, National Institute of Standards, Tersa Street, El-Haram, El-Giza, Egypt*
[b] *Polymers and Pigments Department, National Research Centre, Dokki, Cairo, Egypt*

Natural and synthetic polymeric materials are in high demand that continues to increase year after year, making them essential part of human life. By employing cellulose and cellulose derivatives as fillers for either synthetic or natural polymers, the environmental impact of non-biodegradable materials can be reduced. Nanocellulose (NC) materials have recently gained a lot of interest as potential fillers for reinforcing polymeric materials. The article highlights the different sources of NC, including plant sources, marine algae, bacteria and sea animals. The use of dewaxing solvents, alkali, bleaching agents, enzymes, 2,2,6,6-tetramethylpiperidine-1-oxyl radical (TEMPO), ammonium persulfate (APS), ionic liquids, deep eutectic solvents and steam explosion for pretreatment of lignocellulosic materials was explained. In addition, this review considers the extraction methods, including mechanical fibrillation for the production of cellulose nanofibers (CNF) and acid hydrolysis for the production of cellulose nanocrystals (CNC). Furthermore, the article discusses recent advances in the fabrication of NC polymer composites, such as the melt mixing process, solution casting, 3D printing, electrospinning and pickering emulsions methods. The different characterization techniques of NC polymer composites were discussed in this article. Many promising applications of NC polymer composites, such as sensors, electronics, fuel cells, construction, paper and board, biomedical, food packaging, water purification, aerogels, and hydrogels are considered.
The bibliography includes 299 references.

Contents

Received 3 December 2022

1. Introduction

Petroleum-based polymers have properties that make them ideal raw materials for many applications, such as packaging, construction, consumer products, hygiene products, medical appliances, agriculture, aerospace materials, food, *etc*. The versatility in the applications of petroleum-based synthetic polymers and their resistance to biodegradation will lead to the accumulation of large quantities of them. In turn, this will result in a significant environmental issue at the global level. Furthermore, the price of petroleum oil has increased significantly in recent years.[1,2] Massive amounts of produced and consumed plastic have put life on the Earth at high risk because of its accumulation as a dangerous pollutant. The production of petroleum-based polymers overrides their consumption. For example, in 2018, about 359 million tons of petroleum-based polymers were manufactured compared to 385 million tons consumed, with a difference of about 26 million tons only, which came from the recycling of waste from past years.[3,4] After consumer usage of petroleum-based polymers, only 173 million tons of waste are recycled or landfilled. Due to the poorly disposed and segregated waste, the remaining wastes leak into ecosystems, causing a risky environmental problem. In addition, the release of carbon dioxide arising from the incineration of non-biodegradable polymers will increase the deepening threat of global warming.[5,6] Taking this into account, in 1980, the preparation of biodegradable polymers such as polyhydroxyalkanoate, renewable furan-based materials, polylactic acid (PLA), and poly(butylene adipate-co-terephthalate), started and by now, these materials have been widely researched, manufactured, and used in almost all countries and in numerous aspects of life.[7–12] The number of published papers on NC, and their composites with polymeric materials, is constantly growing. However, as compared to papers addressing other fillers, the number of articles is still modest. According to European plastic data, the ability to produce biodegradable plastic will increase from around 2.1 million tons in 2019 to 2.4 million tons in 2024.[13,14] Cellulose and its derivatives are considered the most abundant biodegradable polymers in nature, which are biocompatible, biodegradable, sustainable and renewable.[15] They make up about one-third of the plant matter. Furthermore, cellulose accounts for $\sim 40-50\%$ of wood, $80-90\%$ of bast fibres such as flax fibers, and $85-97\%$ of seed hairs such as cotton. Cellulose is a straight polymer composed of hundreds to thousands of β-D-Glucose residues, with a degree of polymerization varying from 100 to 15 000 for native cellulose depending on its origin. The β-D-Glucose residues are linked with each other *via* β(1→4) linkages. Furthermore, each glucose residue contains three hydroxyl groups that can be involved in the reaction, giving it a high surface modification capability.[16] The structure of this biopolymer is crucial because it determines how biodegradable, hydrophilic, chiral, and functional cellulose is.[17,18] Due to the intramolecular and intermolecular hydrogen-bonded crystalline domains, cellulose is water insoluble despite the presence of hydrophilic hydroxyl groups. The chemical, biological, and mechanical characteristics of cellulose and its derivatives have received increased attention.[19] Cellulose and its derivatives have been utilized for more than 150 years in a variety of industries, including paper production, biomaterials, food packaging, and the pharmaceutical industry.[20,21] In 1959, prominent physicist Richard Feynman introduced nanotechnology, which had a significant impact on other sciences and technologies. Nanomaterials having unique features such as a significant surface area to volume ratio have been used in energy generation, catalysts, optics, electronics, and medicine. Nanomaterials have a variety of sources, shapes, and sizes, including liposomes, fullerene, dendrimers, graphene, carbon nanotubes, metal nanoparticles, and other shapes.[22,23] Nanocellulose is one of the most promising nanomaterials due to its many appealing factors, such as its non-toxic nature, biodegradability, biocompatibility, high aspect ratio, excellent mechanical capabilities, good optical properties, superior biocompatibility, and tailorable surface chemistry. Recently, NC has become one of the most significant green materials on the market.[24] For these auspicious features, NC and NC based composites have recently gained a lot of interest in a wide range of applications such as sensors, electronics, fuel cells, construction, paper and board, biomedical, food packaging, water purification, aerogels, and hydrogels. Many recent published reviews focused on the preparation methods NC, and its polymer composite characterization and applications. Padhi *et al*.[25] summarized the sources of NC, especially those based on agro waste, and its extraction methods. Dhali *et al*.[26] presented the different extraction methods for different NC materials and applications of its polymer composite. Omran *et al*.[27] demonstrated the different categories of cellulose and process of extracting of each category with limited information about the different sources of cellulose, and its polymer composite applications. Shen *et al*.[28] reviewed the preparation and modification of NC and its polymer composites. All mentioned publications addressed some topics discussed in this review, but none of them covered all aspects that might attract and satisfy the reader who is interested in NC. In this article, we tried to cover adequately the whole area and give a detailed account of data related to NC and its polymer composites, including the different types of NC, its sources, pretreatment and extraction methods. We also presented its polymer composite preparation techniques, characterization methods and its promising applications. The recent published articles (in the last five years) relevant to these topics were considered here. The impact of NC as additives on the properties of different composites was highlighted in different sections.

2. Cellulose categorization

The classification of cellulose has not been universal, but it can be done based on its particle size. It can be categorised into two main types, microcellulose (MC) and NC. Both types are now the most commonly used sizes in industrial applications due to their different properties.[23] Primarily, cellulose can be extracted from plants, algae, bacteria, sea animals, and fungi.[27,29] Microcellulose is usually produced by the partial hydrolysis of the amorphous regions of native cellulose to produce particles with a diameter of 50 μm and a length of $100-1000$ μm [30] and can be categorised into two main types, cellulose microfiber (CMF) and cellulose microcrystal (CMC).[27,31] The latter material has higher mechan-

A.Abdel-Hakim Researcher, PhD, Associate Professor.
E-mail: Ahmedag83@yahoo.com
R.Mourad. Researcher, PhD, Dr.
E-mail: Redamourad14@gmail.com
Current research interests of the authors: biodegradable polymer, nanocellulose, hydrogel and water treatment.

ical properties than CMF and it is the most prevalent type of cellulose derivatives and is extensively used in the food industry. In cellulose extraction, the MC can be converted into NC of different sizes. NC is defined as a cellulosic material having at least one dimension between 1–100 nm.[26] There are three forms of NC: (1) cellulose nanofibers (CNF), also known as nanofibrils or nanofibrillated cellulose, (2) cellulose nanocrystals (CNC) also known as crystallites, whiskers, or rod-like, and (3) bacterial nanocellulose (BNC), also known as microbial cellulose or biocellulose.[32] In comparison to MC, NC has a larger surface area, a higher aspect ratio, a higher strength and elastic modulus, and as a result, a higher reinforcement efficiency, improved surface functionalization, and superior optical properties.[33] CNF is usually produced by pre-chemical treatment followed by exposure to mechanical treatment, while CMF is commonly produced using a chemical treatment.[34] The average diameter of CNF ranges from 20 to 50 nm, while the average diameter for CNC ranges from 5 to 70 nm.[32] The sources of CNF and CNC are usually plants (such as wood, hemp, cotton, flax, mulberry bark and wheat straw) or animals (such as tunicates).[14] Bacterial nanocellulose can be considered as another source of NC. Two main methods of producing BNC include static culture and stirred culture. Despite the longer production time and larger area of cultivation of the static culture, this method is preferable since BNC obtained by static cultures has higher mechanical properties and a higher yield than that produced by stirred culture.[29,35]

3. Nanocellulose sources

Cellulose is made up of hundreds to hundreds of thousands of β(1→4) linked glucose units. Cellulose structure consists of repeating units of anhydroglucose (monomeric units) or cellobiose (a pair of glucose units), with each anhydroglucose unit containing three carbon atoms attached directly or indirectly to hydroxyl groups. The hydroxyl groups are responsible for combining and strengthening the crystalline matrix structure of cellulosic fibrils.[36] Besides cellulose, hemicellulose is another form of polysaccharide in lignocellulosic materials that forms a network with lignin, stabilizing the microfibrillar structures of lignocellulosic materials. In practice, lignin and hemicellulose can be effectively removed by alkaline treatment to produce pure cellulose.[37] The nanocellulose fibers can be obtained through chemical modification such as acid hydrolysis or physical modification such as ultrasonication.[38]

3.1. Plants

Plants are lignocellulosic materials that are cheap, renewable, abundant, and readily available, which makes them a viable supply of cellulose. Jute, hemp, hardwood pulp, cotton, flax, and sisal are just a few examples of cellulose sources that may be processed, harvested, and extracted. In addition, grasses, sugarcane, wheat, cotton stems, and plant parts including stem fruits and leaves are good sources of cellulose.[18] Plant fibers can be classified into wood, leaf, stalk, seed, grass, fruit, and bast (stems) based on their origin. In lignocellulosic materials, cellulose is surrounded by hemicellulose and lignin. High cellulose content, low cost, and low energy consuming chemical extraction should be the main factors when choosing a cellulose source. Aquatic plants such as water hyacinth (*Eichhornia crasspies*) and papyrus have rapid growth where one plant can produce hundreds of plants in one season, and have a short life cycle, and are non-food plants. However, this rapid growth has a negative impact on the environment, blocking streams, lowering water quality, and disrupting aquatic life.[39] Due to the low lignin content (4.1–9%) and its porous structure, water hyacinth (*Eichhornia crasspies*) can be used as a good alternative source for cellulose production.[40,41] Different lignocellulosic materials with their main chemical constituents are listed in Table 1.

Table 1. Chemical composition of various lignocellulosic sources.

Source of lignocellulosic materials	Cellulose	Hemicellulose	Lignin	Ref.
Eucalyptus wood	46.5	14.2	28.3	42
Sugarcane bagasse	58.8	17.7	12.7	43
Corn husk	54.7	27.1	10.4	43
Rice husk	49.6	10.4	21.8	43
Sugar palm fibers	43.90	7.20	33.2	44
Date seeds	31.4	20.92	25.2	45
Sisal fibers	73.8	11.0	9.7	46
Jute fibers	45–63	18–21	21–26	46
Hemp fibers	58.7	14.2	6.0	46
Pine cone	45.3	5.4	39.7	47
Cotton seed hairs	80–95	5–20	0	48
Corn cobs	45.0	35.0	15.0	48
Coastal bermuda grass	25.0	35.7	6.4	48
Switch grass	45.0	31.4	12.0	48
Sunflowers seed hulls	24.1	28.6	29.4	49
Thistle	31.1	12.2	22.1	49
Flax	81	14	3	50
Rice straw	36.2–47	19–24.5	9.9–24	49
Water Hyacinth	57	25.6	4.1	41, 51

3.2. Marine algae

The cell walls of algae are formed of highly crystalline cellulose. Algae can be categorised into three main types such as green, red and brown algae, used to produce cellulose. Red algae have a high carbohydrate content and the ability to hydrolyze into smaller molecules like glucose and galactose, making them a very promising biomass source for a variety of applications. Algae are excellent alternative sources for cellulose and microcrystalline cellulose because they can be grown on a large scale and are environmentally beneficial due to their capability to feed on industrial waste.[52] Their distinguishing features include quicker growth rates compared to traditional plants, simple cell structure, sustainability, biocompatibility, and low growth requirements. Since the cell walls of most algae are free of lignin, cellulose extraction from algae species becomes cheaper and easier. Microcrystalline cellulose (MCC) is produced from algae cellulose, which has favourable chemical characteristics and a high degree of crystallinity.[18] Tarchoun *et al.*[53] used MCC extracted from *Posidonia oceanica* brown algae with a crystallinity index of 74.23%. The prepared MCC had a rod-like structure with an average diameter of 8.4 ± 2.1 μm. In addition, NC was produced from *Gelidium elegans* red algae with an average length and diameter of 547.3 ± 23.7 nm and 21.8 ± 11.1 nm, respectively, with a crystallinity percentage of 73%.[54] The green types, such as *Cladophora sp.* and *Valonia Ventricosa*, were also used to produce NC with a high degree of crystallinity that can reach up to 95%.[55,56]

3.3. Bacteria

Among the potential natural sources of cellulose, bacterial cellulose (BC) has extraordinary properties compared to other cellulosic sources. In many Asian countries, BC is used as a raw material for many food products. The pioneering study on BC was published in 1886.[57] and discussed the production of BC by *Acetobacter xylinum* in the presence of glucose and oxygen. The cellulose obtained from bacteria is pure, in contrast with that obtained from plants, where it is free of lignin, hemicellulose, and pectin. The purity of BC eliminates the need for the chemical purification while also reducing the cost of extraction.[58] The crystalline cellulose found in diverse sources of cellulose has distinct crystal structures, namely in terms of the two crystalline phases: Iα and Iβ which correspond to triclinic and monoclinic unit cells, respectively. The Iα cellulose has higher thermodynamic stability than cellulose Iβ.[59] It was found that plant cellulose is Iβ-rich, while BC is Iα-rich. The BC has higher tensile strength, elastic modulus, degree of crystallinity, relative hydrophobicity, degree of polymerization than that of plant-based cellulose.[60] Due to these properties, BC performs better in such fields as biomedicine, functional devices, water treatment, nanofillers, *etc*.[61] Several aerobic bacteria *e.g*., *Achromobacter*, *Aerobacter*, *Alcaligenes*, *Azotobacter*, *Agrobacterium*, *Komagataei-bacter*, *Rhizobium*, *Pseudomonas*, *Dickeya*, *Sarcina* and *Rhodobacter*, were used in the extraction of BC.[62–65] Bacteria belonging to the *Komagataeibacter genus* are the most extensively studied because they can assimilate a wide range of carbon/nitrogen sources.[66] Bacterial cellulose is formed in the cytoplasmic membrane of bacteria in the form of nanofibrils that aggregate into microfibrils and subsequently, into ribbon-shaped fibrils with an average size of 70–150 nm. BC ribbons are connected in a 3D network, giving this material its own unique properties.[67, 68] According to toxicological studies, BC exhibited no reproductive, embryotoxic, or teratogenic effects. As a result, the US Food and Drug Administration has categorised BC as a safe material since 1992. The main disadvantage of BC is its high production cost.[69] The methods used for producing of BC include the static, stirred and bioreactor culture techniques. A gelatinous membrane of cellulose is produced on the surface of the nutrition solution when the static culture method is used, as shown in Fig. 1, while employing the stirred or bioreactor cultures provide irregular masses, sphere-like structures, or asterisk-shaped structures. The state of the culture environment, which includes the type of bacteria, nutrients, pH, and oxygen delivery, is also important and affects the characteristics of BC. Given that the morphologies and properties of BC produced by different approaches vary considerably, the choice of method depends on the application scenarios.[60] Static culture is the traditional and most commonly used technique for producing BC on a laboratory scale. This technique involves filling containers with fresh nutrient solution, which is then incubated for 1–14 days at the proper temperature (28–30 °C) and pH (4–7). The membranous BC produced from the static method is yellow and needs further purification to turn into a white and pure film, using hot water and sodium hydroxide followed by rinsing with water to reach a neutral pH. Two main problems of the static culture are its low production rate and high production cost.[61] The use of stirred culture has been proposed as a solution to these issues. The production of BC is closely related to the delivery of oxygen, which is recognised as a significant disadvantage of the static culture approach. However, it was demonstrated that a high oxygen supply reduces BC production. The primary goal of designing the stirred culture was to optimise the oxygen delivery to the bacteria during culture. However, it was found that the stirred culture produced the same or a lower quantity of BC over an equal duration. The main reasons for reducing the productivity of stirred culture were the appearance of non-cellulosic material and the genetic instability of bacteria under stirred conditions. The size and shape of the BC produced by stirred culture depend on the rotating speed, culture time, concentration of bacteria, and additive types in the culture medium. The resultant BC has lower crystallinity, a lower degree of polymerization and lower mechanical properties compared to that produced by static culture.[59] Despite these issues, some researches indicate that the stirred culture method may be the best choice for

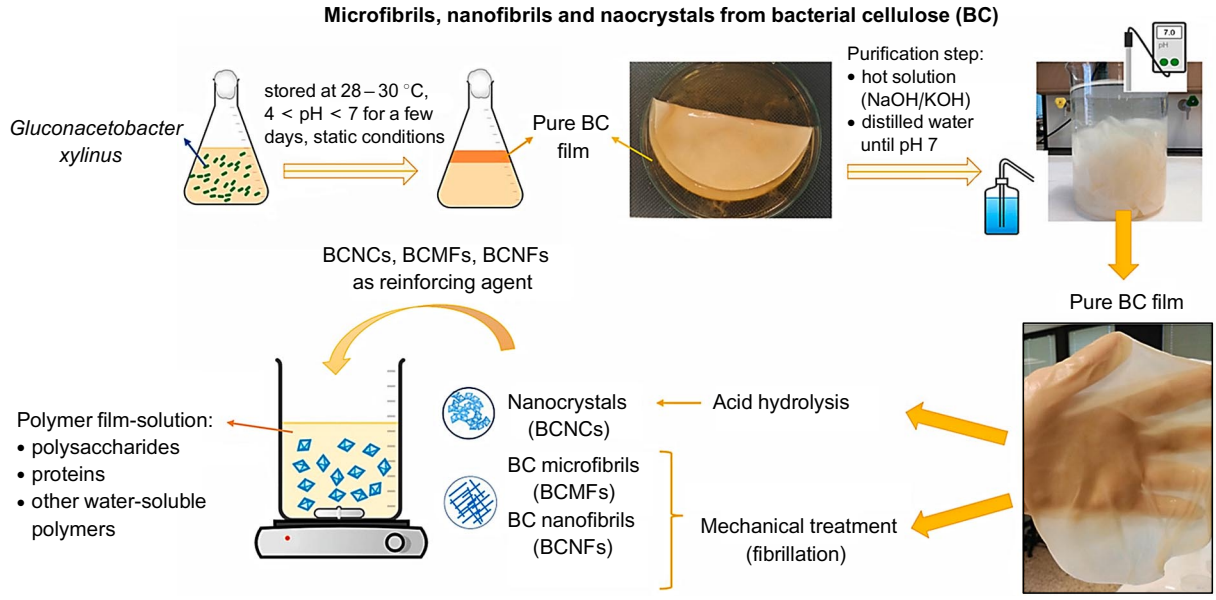

Figure 1. Steps for production of different types of BNC.[69] Published with permission from Elsevier.

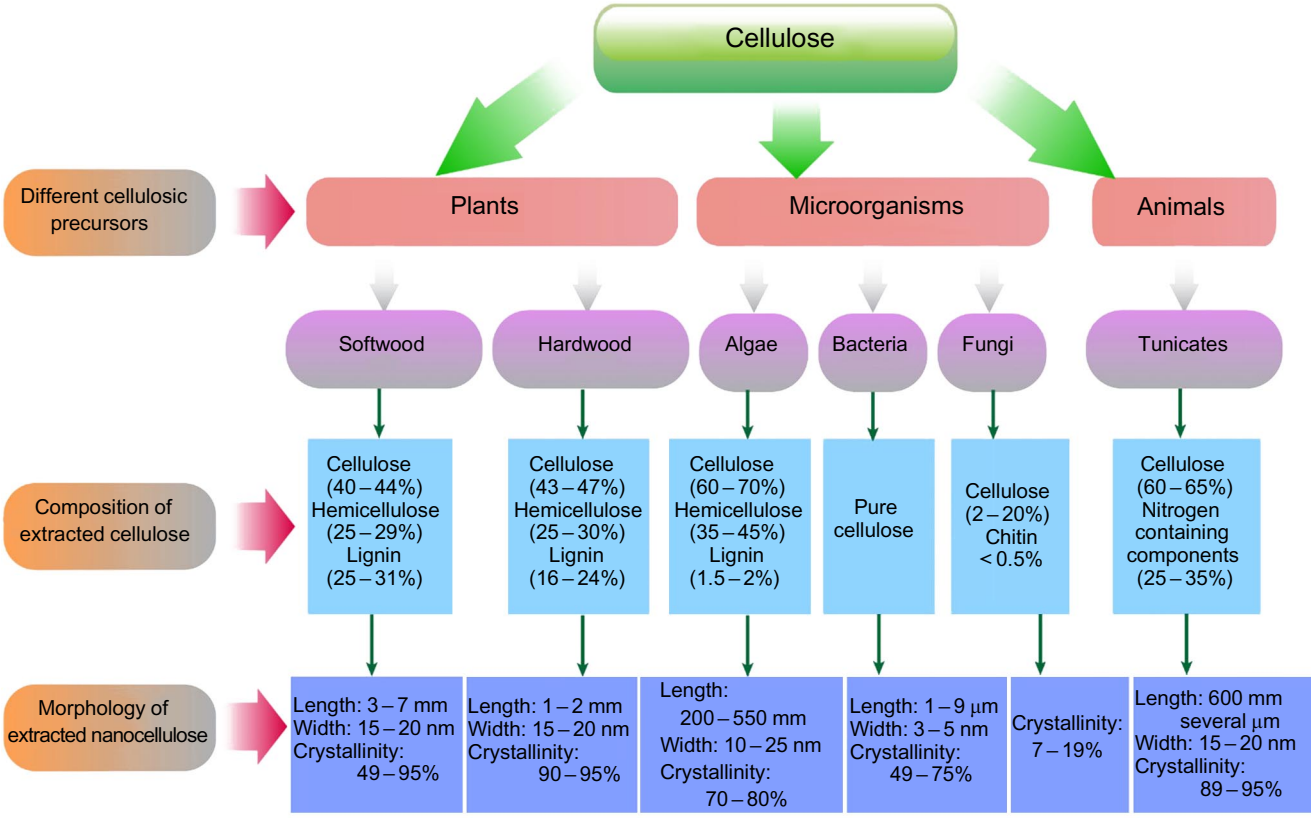

Figure 2. Composition of cellulose derived from different sources and the crystallinity of the isolated NC.[26] Published with permission from Elsevier.

the large-scale, cost-effective production.[70] Based on the foregoing, the stirred culture technique didn't resolve the problems of static culture, and there is a need to develop an efficient production method with low production costs and short culture times. The yield of BC can be improved by continuous cultivation with a high oxygen or nutrient solution transfer rate. High quantities of BC have reportedly been produced by some bioreactor cultures. Recent studies on BC's fermentation and processing technology have introduced some of the province's bioreactor cultures.[71] They can be distinguished by the way they operate, such as creating BC in oxygen-rich air, using a rotating disc, or by supporting biofilms. Oxygen-enriched bioreactors use a stirred tank or airlift bioreactor to increase the oxygen delivery. Airlift bioreactor is more energy-efficient and is characterized by less shear stress than the stirred tank. BC was harvested at the high production rate 2.27 g L^{-1} day^{-1}. A rotating disc bioreactor is another form of bioreactor that allows for the addition of various materials and fibers to the medium and their incorporation into the cellulose to improve the characteristics of BC and BC-based composites. The main purpose of this type of reactor is to generate homogeneous BC. The production rate of such reactor is not significantly higher than that of static culture, which was ~0.24 g L^{-1} day^{-1}.[60] BC can be converted to CMFs, CNFs, and CNCs in suspension or powder form using mechanical or physical methods.

Fungi are considered to be cellulose-producing microorganism, but the content of the produced cellulose is low with a low degree of crystallinity, compared to other sources as indicated in Fig. 2.

3.4. Sea animals

Tunicates are sea invertebrates containing high amounts of cellulose. In tunic tissue, cellulose serves as a skeleton that covers the whole tunicate epidermis. Tunicates use enzyme complexes to generate cellulose.[18] The tunic contains ~60% cellulose and ~27% nitrogen-containing materials as reported by Berrill.[72] Many studies were conducted to obtain tunicate cellulose (TC) using different methods such as prehydrolysis by heating the ground powders with aqueous H_2SO_4 (1%) at 180 °C for 2 h followed by washing with acetone/water (1 : 1, v/v†). Afterward, the washed product was treated with an aqueous solution of Na_2S/NaOH (3/9,%) for 2 h at 180 °C (kraft cooking) and bleached using an aqueous solution of NaClO (3%) for 1 h at 75 °C as indicated in Fig. 3. Tunicates have played a great role in understanding the factors that affect the structure and properties of cellulose.[73] Nishiyama *et al.*[74] studied the crystal structure and the hydrogen-bonding system in cellulose Iβ extracted from tunicate (*Halocynthia roretzi*) using synchrotron X-ray diffraction and neutron fiber diffraction. The results showed that the structure of cellulose Iβ differs from that of cellulose Iα and previous models for cellulose I in having two distinct sheets containing conformationally distinct chains with more complex, disordered and cooperative hydrogen-bonding networks.

4. Production of nanocellulose

The lignocellulosic materials contain cellulosic microfibrils in combination with hemicellulose, lignin and other compo-

† v/v is volume by volume.

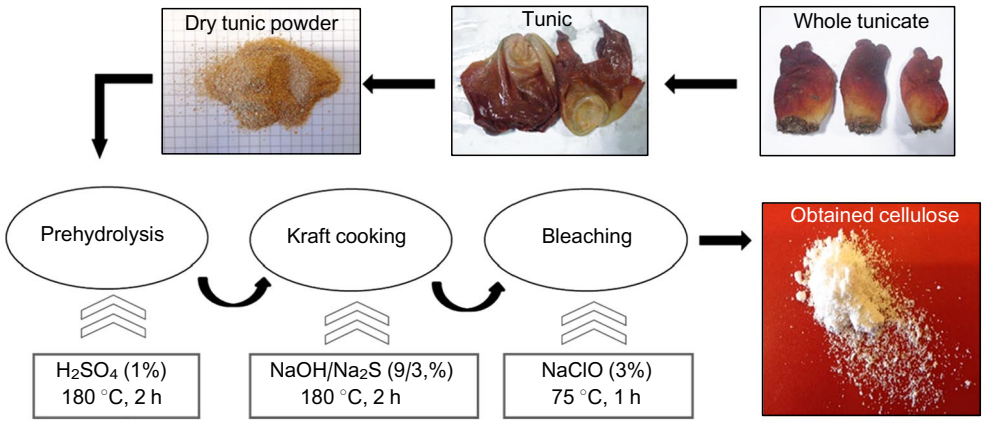

Figure 3. Preparation of cellulose from Halocynthia roretzi.[73] Published with permission from Springer Nature.

nents such as waxes and esters. The amorphous nature of lignin and hemicellulose adversely affects the crystallinity and hence the mechanical properties of the cellulose fibrils. Therefore, removing of cementing materials (lignin and hemicellulose) and other noncellulosic materials is essential to obtain pure cellulosic fibrils with superior properties. The production of nanocellulose is carried out either *via* top-down- or down-top process. The top down process is used to produce CNC and CNF where they are isolated from lignocellulosic biomass. First, the lignocellulosic biomass is chemically pre-treated to remove noncellulosic materials such as waxes, lignin, hemicellulose, and other impurities through dewaxing, alkaline treatment, and bleaching process. The cellulose microfibrils thus obtained is converted either to CNC by acid hydrolysis or to CNF by mechanical treatment as illustrated in Fig. 4.[75] Bacterial nanocellulose is prepared *via* a down-top process where the bacteria produce NC from a low-molecular-weight sugar. BNC is a pure form of NC free of any other components such as lignin, and hemicellulose, so, there is no need for a pretreatment purification process.[76]

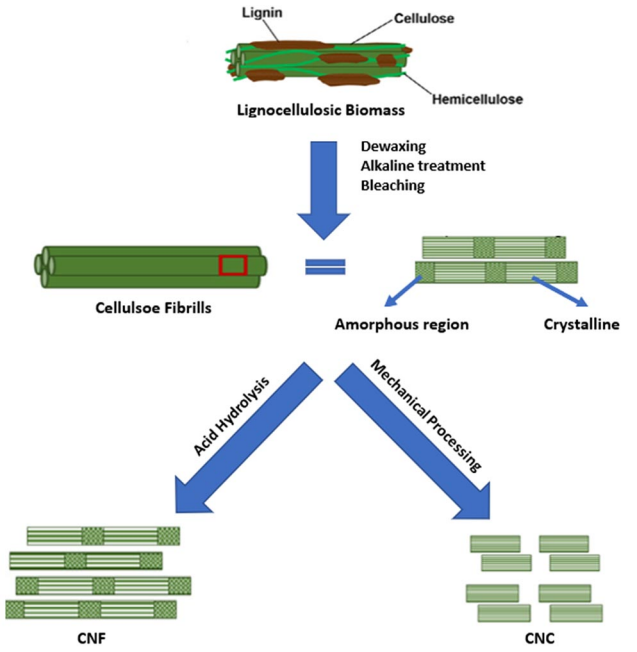

Figure 4. Schematic diagram for production of CNF and CNC from lignocellulosic biomass (top-down process).[75] Published in accordance with the Creative Commons Attribution-Noncommercial license CC BY-NC-ND.

4.1. Pretreatment methods

As mentioned above, different types of cellulose and its derivatives can be identified based on their particle size. CNC, CNF and BNC are the main types differing in particle size, fiber diameter and fiber length. Before the extraction of NC, the pure cellulose should be purified through the removal of waxes, lignin, hemicellulose, and other impurities attached to the cellulose source, followed by bleaching to obtain the pure cellulose.

4.1.1. Dewaxing

The dewaxing process is a pretreatment stage that removes the waxes and extractives contained in the cellulose sources. This can lead to an increase in the Brunauer–Emmett–Teller (BET) surface area of the produced cellulose nanofibers and their pore diameter compared to waxed cellulose nanofibers.[77] Dewaxing using Soxhlet extraction with different solvent mixtures was widely used. In particular, toluene-ethanol, benzene-ethanol, and other solvent mixtures were employed to dewax various lignocellulosic materials (Table 2). The role of a polar solvent such as ethanol is

Table 2. Solvent mixtures used for dewaxing various lignocellulosic sources.

Cellulosic source	Dewaxing chemicals	Temperature, °C	Time, h	Ref.
Cotton	PhMe/EtOH (2 : 1)	90–100	4	77
Bamboo	Acetone/EtOH (2 : 1)	250 (heating element temperature)	2	79
Date Seeds	$CHCl_3$/EtOH (2 : 1)	See [a]	48	80
Coir	PhH/EtOH (2 : 1)	50	72	81
Sunn hemp	PhH/EtOH (2 : 1)	57	2	82
Oil palm	PhH/EtOH (1 : 2)	50	72	83
Sugarcane bagasse	PhMe/EtOH (2 : 1)	50	6	84
Peel of jackfruit	EtOH	See [a]	8	85
Sisal	PhMe/EtOH (2 : 1)	55	12	86
Elaeis guineensis Empty fruit	PhMe/Ethanol (2 : 1)	50	8	87
Tomato peels	PhMe/Ethanol (2 : 1)	See [a]	20	88

[a] Soxhlet apparatus was used.

Table 3. Various alkaline pretreatment reagents and their conditions and effects.[89]

Catalysts	Pretreatment conditions	Major effects	Remarks
Sodium hydroxide	Concentration: 0.5–10% NaOH, T = 60–180 °C, t = 5–60 min, SL = 10–30%	50% hemicellulose dissolution, 60–80% delignification, difficulty in recovery of NaOH	High reaction rate
Sodium carbonate	Concentration: 1–30% Na_2CO_3, T = 60–180 °C, t = 5–60 min, SL = 10–30%	20–40% hemicellulose dissolution, 40–60% delignification, easier recovery than in the case of NaOH	Green liquor
Ammonium hydroxide	Concentration: 5–30% ammonia, T = 30–210 °C, t = 5–60 min, p = 2–17 atm, SL = 10–50%	10–50% hemicellulose solubilisation, 0–80% delignification; no need for washing, low liquid loading (only ~50% moisture is enough)	Ammonia recycle percolation Cost effective
Anhydrous gaseous ammonia	Gaseous ammonia, T = 25–80 °C, t = 72 h, SL ≈ 50%	Mild reaction conditions; no hemicellulose dissolution; no lignin removal	
Liquid anhydrous ammonia	Anhydrous ammonia, T = 70–90 °C, t = 5 min, p = 15–20 atm, SL = 60–90%	Rapid evaporation and liquefaction of ammonia	
Lime	Concentration: 0.05–0.15 g, $Ca(OH)_2$/g of biomass, T = 25–130 °C, t = 1 h–8 weeks, SL = 5–20%	20–40% hemicellulose dissolution, 60–80% delignification, de-acetylation, low energy requirement	Simple and low-cost process

Note. T is reaction temperature, t is treatment time, SL is solid loading, p is pressure.

to remove hydrophilic compounds such as pigments, while nonpolar solvents like benzene (PhH) and toluene (PhMe) facilitate the removal of hydrophobic compounds like waxes and oils. Not only lignocellulosic materials but also cellulosic sources from algae such as *Posidonia oceanica* brown algae were dewaxed using a toluene–ethanol mixture (2 : 1 v/v).[53] In addition, to reduce the heating time, microwave-assisted alkali modification was used in place of the traditional solvent method. In this case, the dewaxing time of *Gelidiella acerosa* algae reduced from 4 h to just 30 min.[78]

4.1.2. Alkaline treatment

Alkali treatment or mercerization includes the exposure of cellulosic materials to aqueous solutions of bases such as sodium hydroxide, potassium hydroxide, ammonium hydroxide and calcium hydroxide.[89] The treatment is usually performed at high temperatures (70–90°C) with mechanical stirring. The alkali treatment using ammonia is preferred because it is easy to recover, non-toxic, and non-corrosive.[90] Also, this treatment is primarily used to promote lignin depolymerization and solubilization, as well as hemicellulose hydrolysis, in order to isolate crude cellulose and make it available for further treatment.[91] However, the process should be controlled to avoid undesirable degradation of cellulose.[92] The hydroxyl groups are transformed to alkoxide ones under the process conditions, resulting in the cleavage of intermolecular ester linkages between hemicellulose and lignin.[93] In this case, the cementing materials used to hold together the cellulosic fibers disintegrate, causing the cellulose fibrils to disperse and expand, altering their shape and mechanical characteristics. Lignin and hemicellulose are partially removed during the alkali pretreatment. Hemicellulose structure is more complicated than that of cellulose, with many branches and acetyl groups predominating. Hemicellulose was shown to have a negative effect on the thermal stability and crystallinity of CNF. The presence of acetyl groups is mainly responsible for the low thermal stability of hemicellulose. In general, the removal of noncellulosic components improves the thermal stability of the extracted cellulose fibrils, making them dense and compact.[94] The conditions and effects of different alkaline pretreatment are shown in the Table 3.

4.1.3. Bleaching

The bleaching process or the delignification step removes the lignin remaining after the alkaline treatment.[90] Bleaching of cellulosic materials is usually performed using hydrogen peroxide (H_2O_2), ozone (O_3), sodium chlorite ($NaClO_2$), chlorine dioxide (ClO_2), or peracetic acid (CH_3CO_3H).[95] The most popular bleaching agent is the acidified sodium chlorite solution. The released chlorine oxide helps to break down hemicellulose and lignin's glycosidic and ether bonds, thereby eliminating any residual lignin.[96] The main disadvantage of chlorine and chlorine derivatives as bleaching agents is that by-products of this process are hazardous pollutants.[97] To overcome this problem, oxygen bleaching,[98] ozone bleaching[97] and peroxy acids[99] were used. Table 4 shows illustrative conditions using these two bleaching agents either alone or in combination with various auxiliary chemicals.

4.1.4. Enzymatic treatment

Enzymatic hydrolysis is a cheap and eco-friendly technique, therefore, it can be used as an alternative mild method for chemical treatment to selectively hydrolyze fibers without excessive degradation of cellulose chains.[96] Cellulase enzyme can hydrolyze part of the cellulose fiber, which facilitates fibrillation. There are five subunits of enzymes, namely, exocellulases, endocellulases, cellobiases, oxidative cellulases, and cellulose phosphorylases, where only endocellulases and cellobiases can catalyse the cleavage of β(1→4) linkages. Enzymatic pretreatment increases the crystallinity of cellulose and causes swelling of the fibers, which is favorable for mechanical treatment.[107] As a result of such processing, the sample swells completely, which reduces the heat produced during mechanical grinding.

Table 4. Bleaching conditions for selected cellulosic sources.

Cellulosic source	Bleaching chemicals	Temperature, °C	Time, h	Ref.
Peel of jackfruit	$NaClO_2$ 1.5% (w/v)	70	120	85
Coconut	5 g of dried fibers were suspended in 150 mL water containing 1.5 g of $NaClO_2$ and 8 – 10 drops of glacial acetic acid	60 – 70	60	100
Curauá and bagasse fibers	acetic acid 0.7% (v/v)/ $NaClO_2$ 3.3% (w/v)	75	240	101
Kenaf	$NaClO_2$ 2%(w/v)/ acetic acid 3% (v/v)	70	180	102
	NaOH 1.5% (w/v)/ H_2O_2 1% (v/v)	70	90	
Rice husk	Buffer solution of acetic acid/ $NaClO_2$ 1.7% (w/v)	100 – 130	240	103
H. sabdariffa	NaOH/acetic acid/ NaOCl mixture	25	60	104
Cotton	$NaClO_2$ 0.1% (w/v)	80	240	77
Tunicate cellulose	NaClO 3% (w/v)	75	60	73
Sugarcane bagasse	Ozone (0.55 g m^{-3})	40 – 85	60 – 360	105
Sisal	Cl_2O/H_2O 1.5 – 2% (w/v)	75	60	106

Note. w/v is weight by volume, v/v is volume by volume.

There are several parameters that control the enzyme efficiency and consequently affect the NC production such as temperature, pH, enzyme concentration and time of hydrolysis. The adsorption/desorption of enzymes over cellulose is mainly controlled by pH of hydrolysis. Typically, the pH between 4 – 5 and temperature in the range of 40 – 50 °C are optimum conditions for cellulolytic enzymes [108] that are basically considered to be mild conditions compared to the traditional chemical treatments. It was found that the hydrolysis time and the enzyme doses obviously affect the morphology of NC. Tong *et al.*[109] studied the effect of hydrolysis time and the enzyme doses of cellulase and xylanase (9 : 1, concentration ratio) on the cellulose nanocrystals (CNCs) morphology. The authors found that at the enzyme dose 10 U and the hydrolysis time of 12 h, rod-like CNCs with a length/diameter 600 and 30 nm, respectively, were produced. With the enzyme dose was raised to 500 U and the hydrolysis time was 5 h, the new spherical CNCs 40 nm in diameter were formed. Also, Chen *et al.*[110] used cellulase enzyme to prepare ribbon-like CNCs from cotton fibers. It was observed that at cellulase doses of 10 – 50 U, hydrolysis time of 5 – 11 h and temperature of 50 °C, the ribbon-like CNCs with the length and width of 250 – 900 nm and 30 – 45 nm, respectively, were obtained, while increasing cellulase doses to the range of 100 – 300 U resulted in the granular form. However, enzymatic treatments require a long time and more expensive reagents compared to acid hydrolysis treatment. On the other hand, the immobilization of enzymes in NC production can reduce the fresh enzymes cost *via* recovering and reusing the enzyme in multiple cycles. Yassin, *et al.*[111] immobilized cellulase in the form of a gel disk by an inexpensive and easy method on carrageenan gel coated with hyperbranched polyamidoamine in the presence of glutaraldehyde. The authors reported that the cellulase gel disk was easy to separate, capable of reusing and retained ~85% of the initial enzyme activity after six cycles. Moreover, the produced CNF from cellulose fibers had a diameter of 15 – 35 nm, a length of several micrometers and enhanced thermal stability. As a result, the immobilization of enzymes can be considered a promising eco-friendly and economic technique for the industrial NC production.

4.1.5. TEMPO oxidation

The 2,2,6,6-tetramethylpiperidine-1-oxyl radical (TEMPO) can selectively oxidise the primary hydroxyl groups (OH6) in the cellulose structure to carboxyl ones under mild conditions. This decreases the interfibrillar hydrogen bonding and increases the mutual electrostatic repulsion, facilitating fragmentation of cellulose microfibers.[112] The presence of catalysts such as sodium bromide and bleaching agents such as NaClO under alkaline conditions is often used for the TEMPO-mediated oxidation treatment. Nanocellulose formed by TEMPO oxidation has higher transmittance and smaller nanoparticle size compared to nanoparticles obtained by conventional hydrolysis method, resulting from the high dispersion of NC in water due to the higher carboxylate content.[113] Although TEMPO oxidation has several advantages such as simplicity, high efficiency and time-saving procedure,[114] it should be realized that TEMPO oxidation is a costly and harmful process.[14] TEMPO was used to oxidize various NC types to expand their abilities and efficiency for more applications. Using TEMPO in oxidation of BNC, for wound dressing application, was optimized to attain high carboxylate content while maintaining a suitable tensile profile. The oxidized BNC was covalently bonded to ε-poly-L-lysine (PLL) *via* the reaction with 1-ethyl-3-(3-dimethyl aminopropyl)carbodiimide hydrochloride/*N*-hydroxysuccinimide (EDC/NHS) after homogeneous distribution by ultrasonication. The TEMPO oxidation treatment improved the antibacterial property of prepared wound dressing and improved the healing rate.[115] TEMPO was used to increase the degree of the silylation reaction (using 3-aminopropyltriethoxysilan) of TEMPO-oxidized NC. The ^{13}C NMR indicated that the silylation reaction occurs not only on hydroxyls, but, more importantly, on the C6′-carboxylic moiety of TEMPO-NC. The increase of degree of the silylation reaction will allow further functionalization to occur under milder conditions.[116]

4.1.6. Ammonium persulfate oxidation

The oxidation process using TEMPO has some limitations, such as high cost, toxicity, a long preparation time, and limited oxidation to C-6 hydroxyl groups. Ammonium persulfate has been extensively used in recent years as an oxidising agent in the hydrolysis of many lignocellulosic fibers.[117] The oxidation process using APS is cost-effective, environmentally friendly, and offers mild oxidation conditions. Also, APS was used to extract NC from the bleached and unbleached pulp isolated from date palm sheath fibers. The optimal oxidation conditions, including the concentration of APS (0.5 – 1.5 M), temperature (50 – 80 °C), and reaction time (8 – 20 h) were found. The highest carboxyl content was obtained at 1.25 M of APS with a reaction time of 16 h and at 1 M of APS with a reaction time of 10 h,

respectively, at 60 °C and 1 : 100 liquor ratio for both products.[118] Wang *et al.*[117] used APS swelling (3 h, 25 °C a solid – liquid ratio of 1 : 50) followed by oxidation of C-6 hydroxyl groups (60 °C) to extract CNC from cotton linters. The CNC yield was 95.75%, with zeta potential value of 30.5 mV and crystallinity index of 83.51%. Marwanto *et al.*[119] used APS to extract CNC from balsa and kapok fibers by a one-step procedure without pretreatment. The prepared CNC has a diameter in the range of 1.25 – 11.87 nm depending on the fiber type and the APS concentration, with a maximum crystallinity index of 81.03%.

4.1.7. Ionic liquids

Some ionic liquids (ILs) are capable of solubilizing lignocellulose, the property being essential for biomass pretreatment. The cellulose may be easily precipitated with an anti-solvent, and the anti-solvent must be removed in order to recover and recycle the ILs. They have many advantages compared to organic solvents, such as negligible vapour pressure at ambient temperature as well as high thermal stability, making them ideal solvents for cellulose extraction. Ionic liquids can be composed of a mixture of small inorganic/organic anions and large organic cations. ILs may consist of more than one anion or cation. The melting point of many ILs is below 100 °C and many of them are liquid at the ambient temperature. Both cations and anions can disturb the noncovalent bonds in the cellulosic structure.[120] The cations may include azolium (*e.g.*, triazolium, imidazolium), pyrrolidinium, alkylammonium, phosphonium, pyridinium, *etc.* Anions may include both inorganic anions (*e.g.*, halide, perchlorate, sulfate, nitrate, nitrite, azide, hexafluorophosphate, tetrafluoroborate), and a number of organic anions (*e.g.*, sulfacetamide, triflate, benzoate, alkylcarbonates, alkylsulfates, organic carboxylates). ILs can selectively solubilize lignin and hemicellulose. 1-Ethyl-3-methylimidazolium acetate ([EMIM][CH_3COO]) was used as an IL in the recovery of cellulose, lignin and hemicellulose in pure form. In addition, the ILs were effectively recovered and reused.[121] 1-Butyl-3-methylimidazolium chloride [BMIM][Cl] and 1-ethyl-3-methylimidazolium acetate [EMIM][CH_3CO_2] were used to solubilize the shells of peanuts and chestnuts. The results showed that [BMIM][Cl] was less effective in dissolution than [EMIM][CH_3CO_2]. In addition, [EMIM][CH_3CO_2] recovered 75% and 95% of cellulosic material from peanut and chestnut shells, respectively.[122] 1-Ethyl-3-methylimidazolium chloride [EMIM][Cl] and 1-propyl-3-methylimidazolium chloride [PMIM][Cl] were used to recover CNC from two types of MCC (Avicel and Sigmacell) with an average particle size of 20 nm for Avicel and 100 nm for Sigmacell.[123] Figure 5 shows some examples of cations and anions in ILs.

4.1.8. Deep eutectic solvents

The main drawbacks of ILs are their high toxicity, impurity, laborious synthesis, non-biodegradability, and high cost of raw materials. Deep eutectic solvents (DESs) are a new generation of solvents that can overcome disadvantages of ILs, since they can be prepared by simply mixing two cheap, biodegradable, and safe components.[125] These two components can form an eutectic mixture where the product has a melting point lower than the starting materials. DESs are prepared by mixing a hydrogen bond acceptor (HBA) compound (such as quaternary ammonium salts) with a

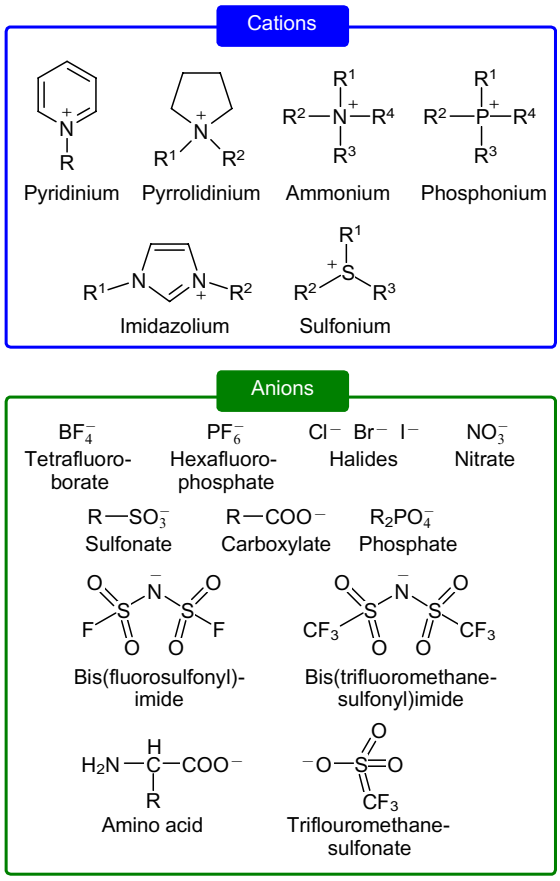

Figure 5. Examples for cations and anions in ILs.[124] Published in accordance with the Creative Commons Attribution license CC BY 4.0.

hydrogen bond donor (HBD) compound, such as ethylene glycol, glycerol, amino acids, organic acids and sugars.[126] Zhang *et al.*[127] prepared a series of DESs consisting of the most common HBA, namely, choline chloride (ChCl), with various HBDs such as glycerol, urea, citric acid, and oxalic acid (Fig. 6). The most effective DES for dissolution cellulose was oxalic acid/ChCl.[127] ChCl and lactic acid (1 : 9 molar ratio) were used to extract nanocrystalline cellulose from Moso bamboo using a solid: liquid ratio of 1 : 25. The extraction percentage was 91% (120 °C, 3 h).[128] Also, ChCl-urea (molar ratio of 1 : 2) was used as DESs to extract NC with a high percentage (90%) *via* heating with DES at 100 °C for 2 h.[129]

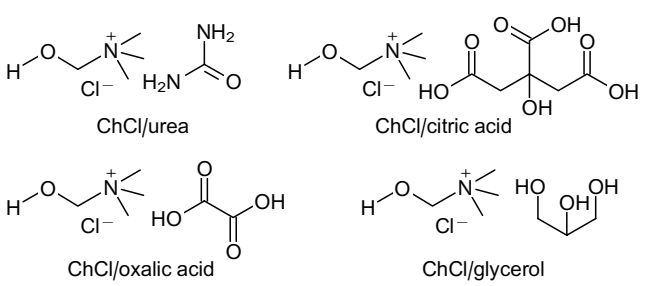

Figure 6. Some examples of DESs based on ChCl as HBA with different HBD.[127]

4.1.9. Steam explosion

Steam explosion is a hydrothermal pretreatment, in which lignin is depolymerized, and cellulose fibrils are exploded when exposured to high pressurized hot steam. This method has been widely used because of its low-energy and chemical consumption. The biomass is treated with steam at a high temperature (160–280 °C) and under a high pressure (0.7–4.8 MPa). Cellulose fibrils, lignin and hemicellulose are hydrolyzed due to the evaporation of water contained in the material followed by its rapid expansion. Note that hemicellulose hydrolysis can produce a lot of organic acids, by which assists the hydrolysis process. The key parameters in improving the efficiency of the steam explosion are high temperature, acidic conditions, and the use of catalysts such as SO_2, H_2SO_4 and CO_2. Tanpichai *et al.*[130] investigated the effect of steam explosion pressure and treatment cycle number on the properties of the extracted microfibers. It was found that lignin and hemicellulose can be partially eliminated improving thermal stability and crystallinity percentage of the product. In addition, using five cycles of steam explosion and under pressure of 20 kgf cm^{-2} ($\sim$2 MPa), lower width (3 μm) and length (93 μm) were recorded in the extracted fibers compared to the original fiber (width of 45.8 μm and length of 2 cm). The authors hypothesized that with more cycles of the steam explosion, more nanofibers could be extracted. The effect of hydrothermal pretreatment, temperature, and number of depressurization cycles on the properties of CNF extracted from garlic skins was investigated. The highly crystalline CNF with a higher aspect ratio and good thermal stability was obtained at 130 °C and 5 depressurization cycles.[131] CNF with a diameter of 10–20 nm was extracted from pineapple pomace using different acid hydrolysis (oxalic and sulphuric acids). The steam explosion pressure and steaming time have a great influence on the properties of extracted NC. Different pressures and steaming times were applied (30 atm/5 min, 35 atm/5 min, 40 atm/5 min, and 35 atm/15 min) to the Japanese cedar. The highest tensile strength and elastic modulus of the extracted CNF was obtained at 35 atm/5 min. Furthermore, the molecular weight of the cellulose decreased as the severity of the steam explosion increased (35 atm/15 min).[132] The effect of different temperatures (195, 200, 205, and 210 °C) and steaming times (5, 10, and 15 min) on the isolation of CNF from sugarcane bagasse waste was studied. The best steam explosion conditions were 205 °C and 5 min of steaming time. The cellulose microfibers were changed to CNF with a diameter 3–7 nm after defibrillation using high-pressure homogenization method.[133]

4.2. Extraction of nanocellulose

Several methods have been developed for the extraction of NC from cellulosic materials, allowing the production of cellulose of different types, sizes, and properties.[134] The different techniques for the extraction of NC are listed below.

4.2.1. Acid hydrolysis

The acid hydrolysis method has been widely used in the extraction of NC from cellulosic sources. Acids can hydrolyse the disordered regions in cellulose chains while the ordered parts remain intact, increasing the crystallinity of the produced NC.[135] Sulfuric acid is the most common acid used for acid hydrolysis.[136] It helps to isolate NC and disperse it as a stable colloid system *via* esterification of the hydroxyl group by sulfate ions.[137] The main factors affecting the properties of the obtained NC are temperature, reaction time, and acid concentration. The main disadvantage of acid hydrolysis is the acidic wastewater generated from neutralisation through continuous washing and centrifugation of the suspension up to neutral pH.[102] The obtained suspension can be neutralised using an alkaline solution. Maiti *et al.*[138] extracted NC from different biomass by sulfuric acid (47%) hydrolysis followed by washing with deionized water, centrifugation, alkaline neutralisation with 0.5 N sodium hydroxide and washing again with distilled water. Tarchoun *et al.*[139] used various acidic solutions (HCl, HNO_3, H_2SO_4, HCl/H_2SO_4 (2 : 1, v/v), and HCl/HNO_3 (2 : 1, v/v) in the acid hydrolysis of giant reed. The highest yield, greater crystallinity index, and the smallest dimension were obtained with mixed acid hydrolysis instead of single acid hydrolysis.

4.2.2. Mechanical process

The mechanical extraction method involves the application of high shear force to cleave the cellulosic fibrils in the longitudinal axis to isolate the fibrils as a nanofibrillated cellulose. The most common mechanical methods used in these approaches are high pressure homogenization, ball milling and ultrasonication methods.[140]

4.2.2.1. High pressure homogenization

High pressure homogenization is carried out by exposure of cellulose slurry to high pressure and high velocity.[141] The shear force, pressure influence, and shear force in fluid are generated to cleave cellulose microfibers into nanometer size in diameter. Li *et al.*[142] used pretreatment of sugarcane bagasse with ionic liquid (1-butyl-3-methylimidazolium chloride ([BMIM]Cl)) followed by high pressure homogenization to extract NC with diameter of 10–20 nm with decreasing the crystallinity compared to the original cellulose. Wang *et al.*[143] used high pressure homogenization after dissolution in [BMIM]Cl to extract NC from eucalyptus pulp, and the obtained NC had a diameter of 20 nm and decreased thermal stability and crystallinity. The decrease in crystallinity is due to the breaking of the intermolecular and intramolecular hydrogen bonds present in the cellulose structure as a result of exposure to the high pressure homogenization process. Ni *et al.*[144] used high-pressure homogenization after acid hydrolysis of ginkgo seed shells, where the NC length decreased from 1500 to 406 nm after raising the homogenization pressure from 10 to 70 MPa. Three types of non-wood NC were prepared from cotton linter, sisal, and bamboo by TEMPO-mediated oxidation followed by high pressure homogenization. It was found that the chemical composition and morphology of different produced NC were almost similar, with a difference in size and crystallinity. The highest crystallinity index (89.3%) and the lowest size (464 ± 326 nm) were recorded for the sisal source.[145]

4.2.2.2. Ultrasonication

Ultrasound is sound waves in the frequency range of 20 kHz–10 MHz that can be produced by a transducer in which mechanical or electrical energy is converted to high-frequency acoustical energy. The impact of ultrasonic can disrupt the relatively weak bonds between cellulose fibrils (*e.g.*, hydrogen and van der Waals) causing disaggregation and defibrillation of aggregated fibers to produce NC.[146] It can be used alone or in a combination with acid hydrolysis.

The NC was isolated from pulped, bleached, and acid hydrolyzed hyacinth fiber by sonication at 600 W for 1 h. The produced NC had an average diameter and length of 15 and 147 nm, respectively.[147] The purified and bleached Douglas Fir fibers were subjected to ultrasonication at 20 kHz for varying times (30–60 min). The crystallinity index reached to 71.46% for bleached fiber that was sonicated for 30 min at amplitude of 40% with an average diameter 10–50 nm (for 66% of fibrils).[148]

4.2.2.3. Ball milling

Shear forces are produced between the balls and between the balls and the jar's surface as a result of the centrifugal force from the revolving jar. The diameter of the cellulose fibrils decreases due to their cracking. Many factors affect the size of milled cellulose, such as the size and number of balls, the milling state (dry or wet state), the solvent used, the milling speed and time and the ratio between the weight of balls and materials' weight.[149] Ago *et al.*[150] reported that there is a significant effect of the amount of water present in the milling jar on the changing of the crystalline structure by the friction force generated from ball milling, where with the presence of 30% water, the cellulose derived from cotton is converted from cellulose type I to type II (more stable) while dry grinding changes it to an almost amorphous state. The main drawback of ball milling is its negative effect on the cellulose crystallinity, so it is preferred to be used as a pretreatment technique prior to hydrolysis. The main disadvantage of the mechanical process is its considerable energy consumption and therefore, it is typically paired with another pretreatment technique to reduce the energy consumption.[141] Figure 7 shows the influence of mechanical and acid hydrolysis on the defibrillation of agglomerated cellulose fibrils.

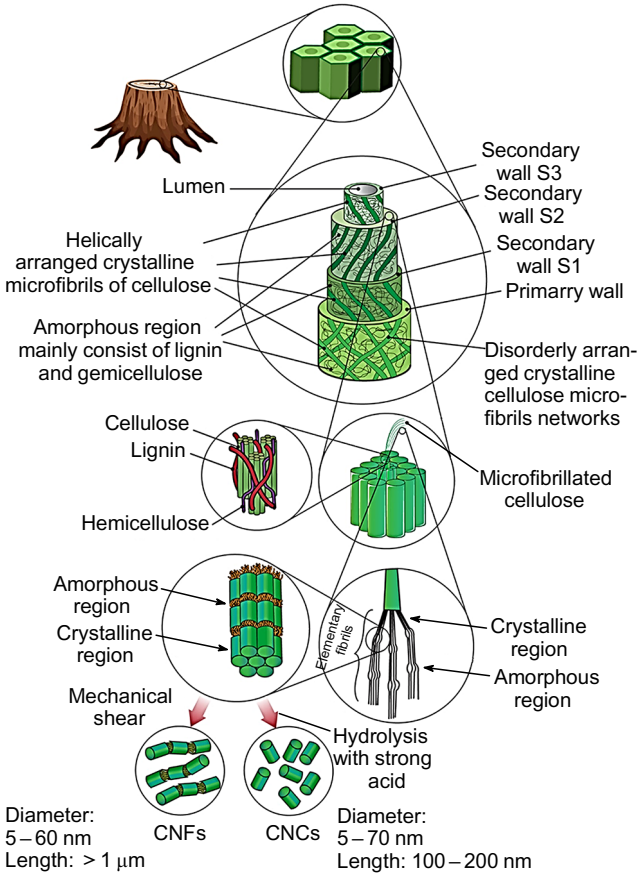

Figure 7. The effect of acid hydrolysis and mechanical treatment on the defibrillation of cellulosic materials.[26] Published with permission from Elsevier.

5. Nanocellulose polymer composite preparation methods

Nanocellulose can be used to reinforce natural or synthetic polymers to produce a composite having different properties compared to its individual components. Thermoplastic polymers can be converted into a viscous liquid with an increase in temperature, which can be moulded into different shapes. These melting and shaping processes can be repeated many times, causing a decrease in the molecular weight of the polymer and, consequently, a deterioration in the polymer properties. As for thermosetting polymers, they cannot be melted or reprocessed after curing due to the formation of cross-linking. The different nature of NC (hydrophilic) and thermoplastic or thermosetting polymers (hydrophobic) causes incompatibility between them. Therefore, some chemical or physical modification should be performed to improve the interfacial adhesion between the matrix and filler. There are two main methods for producing cellulose polymer nanocomposites: melt processing and solution casting. Other methods, such as electrospinning, 3D printing, Pickering emulsion, and *in situ* polymerization should be mentioned. In some cases, a combination of these two or three methods may be used.

5.1. Melt mixing process

Cellulose nanocomposites can be manufactured mainly by the melt mixing process using a cascade of extrusion and an injection moulding or compression moulding or using Brabender Plasticoder internal mixer followed by compression moulding. The extrusion and melt mixing processes

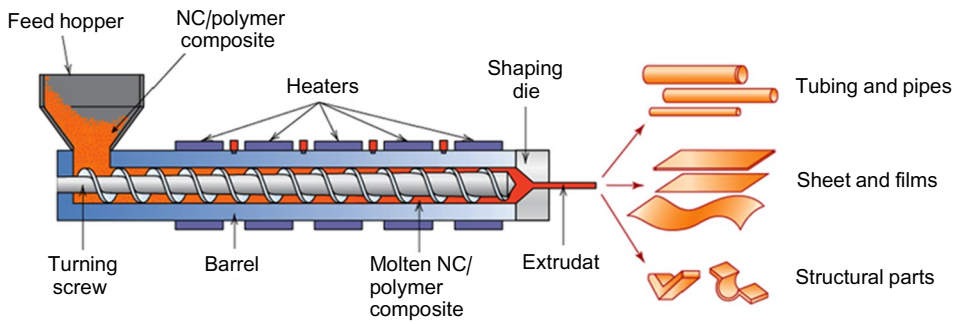

Figure 8. Preparation of NC/polymer composite *via* extrusion process.[153] Published in accordance with the Creative Commons Attribution license CC BY 4.0.

(Fig. 8) are commonly used to improve the nanofiller dispersion in composites, which have a positive effect on their mechanical properties. The extruder consists of screws, heating elements with different heating zones, and dies, while the Brabender Plasticoder internal mixer comprises screws and one heating zone. The function of the screw in an extruder is the mixing of polymer, filler, and other ingredients and transporting the mixture from the feeding zone to the die, while in the Brabender Plasticoder internal mixer, the screw is for mixing only.[151] The viscosity of the molten composite plays an important role in the dispersion of the filler within the polymeric matrix, where the best dispersion of filler and less aggregated filler is obtained while reducing the viscosity of the molten composite. The viscosity can be reduced by high temperatures or by high shear rates. Before the melt mixing process, the thermal stability should be monitored using thermogravimetric analysis (TGA), while the mixing temperature shouldn't be higher than the initial decomposition temperature of the composite.[152] The shear force generated from the screw can break the bonds between NC particles and prevent their agglomeration. In addition, the mixing time should be carefully selected to avoid the degradation of the composite component, which may adversely affect the properties of the final product.[141]

5.2. Solution casting

Solution casting is the most common and simple technique in the processing of cellulose nanocomposite.[154] For water soluble polymers, the interaction between the polar polymers and the dispersed polar cellulose filler is strong. After mixing these two components, a suspension is obtained, from which the solid nanocomposite is produced through casting in the mould followed by solvent evaporation as described in Fig. 9. Nanocomposite reinforcing action on the polymeric matrix primarily depends on the formation of a percolating network between NC molecules *via* hydrogen bonding. The slow processing technique allows the reorganisation of NC molecules and induces the formation of percolating networks.[155] For water insoluble polymers such as polypropylene, polyethylene, and polylactic acid (PLA), it is very important to prevent NC aggregation due to the incompatibility between the hydrophilic cellulose filler and the hydrophobic polymeric matrix. Several strategies were used to improve the dispersion of NC in hydrophobic matrixes, such as using a surfactant as a dispersing agent, including one part compatible with the hydrophilic NC (head of the surfactant) and the other with the hydrophobic polymer (tail of the surfactant). Another strategy is to modify the cellulose surface by grafting or the sol–gel process to reduce its hydrophilicity to improve interaction with the hydrophobic polymer.[154]

5.3. 3D printing

Three-dimensional (3D) printing, known as additive manufacture technology, is a process that can be used to produce a three-dimensional object from predesigned 3D models created by computer-aided design (CAD) software. 3D printing has numerous advantages, including: (i) rapid prototype production; (ii) simple technique; (iii) flexibility and opportunity for innovation; (iv) low material consumption; and (vi) fine control over the porosity of composites. The objects created by 3D printing have good chemical, mechanical, and thermal properties.[156] This methodology was used to create PLA/CNF composite, where the incorporation of 1% CNF in to the PLA matrix improved both elastic modulus and tensile strength by 63% and 84%, respectively. In addition, the incorporation of CNF decreased the void contents in the 3D printed PLA/CNF composite without significantly changing its thermal stability.[157] Palucchi Rosa *et al.*[158] prepared a composite of poly(ethylene glycol) diacrylate (PEGDA) and acrylated epoxidized soybean oil (AESO) containing CMC or CNC by 3D printing technique. The elastic modulus increased by 890% after incorporation of 2.4% CMC, while the tensile strength increased by 59% after addition of the same quantity of CNC. Moreover, the contact angle decreased after the addition of CMC and CNC. Zhou *et al.*[159] used 3D printing to prepare a shape memory polyurethane/CNC composite. The shape recovery rate was enhanced by 99% after adding CNC. In addition, the tensile strength was improved by 71% after the addition of CNC compared to neat polyurethane.

5.4. Electrospinning

Electrospinning is a flexible method for producing fibers of uniform diameter and length ranging from 0.1 micrometre to several micrometres. This method involves, as represented in Fig. 10, the use of a high voltage source to

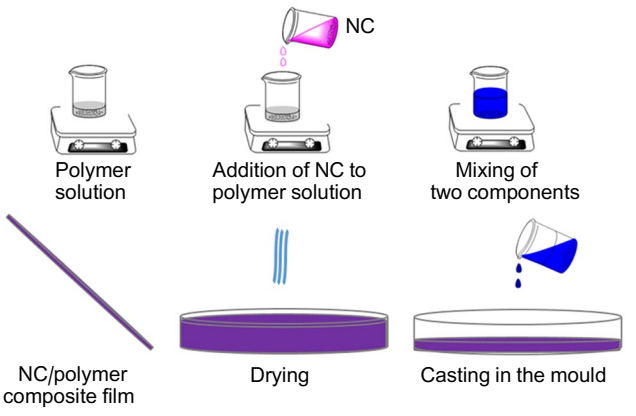

Figure 9. Solution casting technique for preparation of NC/polymer composite.

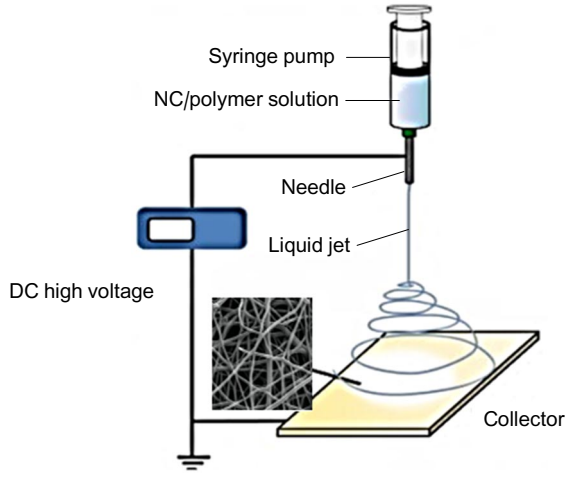

Figure 10. Preparation of NC/polymer composite using electrospinning technique.

stimulate the creation of a liquid jet. The nanofibers are formed by feeding a viscous solution or molten polymer into a syringe needle or capillary tube in an electrical field. The fibers are continuously stretched by the electrostatic repulsion between surface charges and after the solvent evaporation, the dry fibers are formed.[160] Ashori *et al.*[161] prepared poly(ether sulfone) (PES)/CNC nanocomposite membranes using electrospinning technique. The resultant membrane showed many interconnected voids, high hydrophobicity, which caused higher water flux. Ge *et al.*[162] used electrospinning to fabricate CNC/waterborne polyurethane/polyvinyl alcohol nanofiber film with excellent porosity performance. The amount of CNC had a great effect on the processability and porosity of the film formed, with 1% CNC resulting in the best spinability and the highest porosity percentage (62.61%). CNC/Polyvinylidene fluoride composite was obtained using electrospinning technique. The produced nanofiber exhibited excellent oil absorption where the adsorption capacity for engine oil reached 73.04 g g^{-1}. The incorporation of CNC to the polyvinylidene fluoride enhanced the mechanical properties significantly.[163] Electrospinning was widely used for the fabrication of many composites, such as CNC/polyamide 6,[164] NC/polyvinyl alcohol (PVA),[165] and cellulose acetate/CNC.[166]

5.5. Pickering emulsion

Pickering emulsion is an emulsion system, in which the dispersed phase is stabilized by solid particles. This emulsion type is more stable than that stabilized by surfactant and thus offers a wide range of applications. Among these solid particles used to stabilize Pickering emulsion, NC was used due to its amphiphilic character, renewability, biodegradability and biocompatibility.[167–169] Biswas *et al.*[168] used NC as a solid stabilizer for hydrophobic 2,2-bis[4-(acryloxypolyethoxy)phenyl]propane (ABPE-10) acrylic resin in water followed by vacuum filtration on a PTFE filter and drying at 40 °C overnight to obtain a NC/resin mat. The dried mat was compression moulded at 150 °C and pressure of 2 MPa for 5 min. The prepared nanocomposite had excellent transparency and high thermomechanical and thermo-optical stability compared to other cellulosebased transparent materials. CNF/polystyrene (PS) nanocomposite was prepared using Pickering emulsion, where the styrene monomer was dispersed in an aqueous suspension of CNF followed by dissolution of the initiator. The suspended mixture was ultrasonicated to form high stable Pickering emulsion, which underwent polymerization after heating at 70 °C to form PS nanoparticles stabilized by CNF. The CNF/PS nanocomposite sheet was obtained after filtration. The low transparent CNF/PS nanocomposite sheet can be converted to high transparent film *via*

Table 5. Preparation methods for various NC polymer composites.

NC source	Composite	Preparation technique	Effect of NC	Ref.
Saw dust	CNF/PLA/polybutylene succinate (PBS)	Twin-screw extruder and 3D printing	The CNF extracted was chemically modified using canola oil. The modified CNF/PLA-PBS composite showed an increase in tensile strength and modulus by 40% and 30%, respectively	170
Bleached wood pulp	PBS / MCC/CNF	Brabender mixer (melt mixer) at 140 °C	The thermal stability was improved for cellulosic filler after incorporation into the PBS matrix. The crystallinity decreased after addition of cellulosic filler. The Young modulus and storage modulus increased whereas the tensile strength decreased. The composites containing cellulose filler showed improved starting biodegradation	171
Oil palm	Polypropylene/cyclic natural rubber/MCCs and(or) CNFs	Brabender mixer (melt mixer) at 180 °C followed by compression moulding at 190 °C for 10 min	CNF improved tensile strength, elastic modulus and thermal stability to more extent than MCC. The interphase surface tension improved after addition of cellulose fibers	172
Pineapple leaves	Natural rubber (latex)/MCC and(or) CNCs	Mechanical stirrer followed by mould casting	The dispersion of CNCs within the Natural rubber was the best at 2.5 phr.[a] The highest tensile strength was observed at 2.5 phr of CNCs	173
Tunicin	CNCs/epoxy resin	Magnetic stirrer followed by solution casting	Improved adhesion between CNCs and epoxy matrix resulting in improved tensile strength. CNCs improved dynamic mechanical properties of epoxy matrix	174
Bamboo	Polyvinyl alcohol/starch/CNF	Mechanical stirring using homogenizer followed by solution casting	The addition of CNF increased the melting temperature by 6%, melting enthalpy by 23% and crystallization enthalpy by 55 compared to the PVA/starch control blend. The tensile strength and elongation at break increased by 24 and 51%, respectively, compared to the control blend	175
Helicteres isora Plant	Poly(butylene succinate)/CNF	Melt mixing using Brabender twin-screw	Tensile and flexural strengths showed an increase up to 1.5 phr of CNF	176

Table 5 (continued).

NC source	Composite	Preparation technique	Effect of NC	Ref.
Nata-de-coco	Polyhydroxyalkanoate (PHA) and PLA with CNCs or MFC	Co-rotating twin-screw extruder for mixing and solution casting for film formation	The reinforcement with MFCs improved the tensile strength and modulus to more extent than CNCs. The roughness of the MFC reinforced polymer is higher than that of the CNCs reinforced one and neat polymers, which improves the interlaminar bonding between multilayers in case of MFC reinforced polymer	177
Bleached pulp board	Polyhydroxybutyrate(PHB)/ CNF or CNCs	Dissolution in $CHCl_3$ followed by coating on glass plate using film applicator	Barrier properties of the CNF/PHB composite decreased and then increased with increasing of the CNF content. Similar behaviour was observed for CNC/PHB. After addition of 1% CNC to PHB, the elongation at break and Young's modulus of CNCs/PHB composite film increased by 91.2% and 18.4%, respectively, while the tensile strength decreased by 3.5%. Both elongation at break and tensile modulus decreased with increasing CNF content in the CNF/PHB composite	178
CMF and CNF	(NCs)/poly(aryl ether ketone) (PAEK)	Pickering emulsion	CMF and CNF stabilized the Pickering emulsion of the PAEK and improved the thermal insulation of the prepared (NCs)/poly(arylether ketone) aerogel, which showed efficiency of 98.1% in diphenylamine removal from water	179
Wood pulp	PLA/regenerated cellulose (RC) nanocomposites	Pickering emulsion	The PLA/regenerated cellulose composite was prepared using Pickering emulsion to achieve the maximum homogeneity. The amount of RC was changed from 0 to 3 wt.%	180
NC	NC/Starch nanocomposite	Electrospinning	Cationic starch (CS) was used as binding agent between starch and NC. The most effective ratio of cationic starch: NC on the mechanical properties of the fibres was 1 : 1 and 2 : 1 at their best concentration (2%, w/w of starch)	160
	NC/PVA	Electrospinning	The maximum hydroxyl value, and the minimum values of crystallinity and fibres' diameter were obtained at 6% NC. The maximum tensile was obtained at 2% NC	165
CNC & CNF	CNC/citric acid (CA)/CNF	3D printing	Citric acid was used as a crosslinker for the cellulosic layers. The best formulation was (CNC : CA : CNF = 20 : 2 : 1), which improved layers interfacial adhesion, while flexural strength modulus was improved by 128%	181
Oil palm biomass	CNF/$CaCO_3$	3 D printing	The 3D printing was used to prepare pours composite for drug delivery application. The presence of CNF allows to control the drug release over 24 h	182

[a] phr is parts per hundred rubber.

hot pressing at 160 °C for 30 s. Table 5 shows several preparation methods for various NC polymer composites.

6. Nanocellulose polymer composite characterization

6.1. Mechanical properties

Nanocellulose has a high specific surface area, providing good interfacial adhesion between the cellulosic filler and the polymer matrix. Therefore, NC can be used to reinforce various polymers. The effectiveness of the reinforcement of any filler depends on its particle size of the filler, the interfacial adhesion between the filler and the polymer matrix, and the dispersion of the filler in the polymer matrix. In general, the optimum concentration of nanofiller should be determined, which provides whereby the best distribution of the filler and the strongest interfacial adhesion between filler and polymer matrix. Increased nanofiller concentration will cause agglomeration in the filler, reducing interfacial adhesion in the composite and, as a result, mechanical properties.[183, 184] Moreover, the agglomeration of nanofiller will cause a non-uniform distribution of the

filler in the polymeric matrix, which is negatively reflected on the stress distribution within the composite, resulting in a decrease in the mechanical properties.[146] The mechanical properties of the NC polymer composite can be evaluated through the measurement of tensile strength, tear strength, peel strength, compressive strength, hardness *etc*. and dynamic mechanical properties namely, storage modulus, loss modulus, and damping factor.

6.2. Thermal properties

The thermal properties of the NC polymer composite are very important in selecting a particular application of the composite. The thermal properties characterizing the composite include melting point, crystallisation temperature and glass transition temperature (Tg), which can be determined by deferential scanning calorimetry (DSC). The hydrogen bonding between cellulosic filler and polymeric matrix can increase the Tg of the composite due to restriction of segmental motion.[185] The thermal stability of the composite at different temperatures should be investigated using TGA, with the sample subjected to a gradual increase in temperature and the weight loss assessed as an indicator of the material degradation. In general, the presence of enormous oxygen content in cellulose filler decreases its thermal stability.[186] Due to the complex network structure formed in the cellulose nanocomposite at a low concentration of nanocellulosic materials, the thermal stability of the nanocomposite can be improved. At higher concentrations, the thermal stability may be decreased as a result of filler agglomeration.[187]

6.3. Barrier properties

The crystalline nature of NC and their ability to form a percolating network with the polymeric matrix decrease the permeability of NC polymer composites through increasing the tortuosity path for the diffusing molecules. Also, hydrogen bond formation between NC and the polymeric matrix will restrict the polymer chain movement, resulting in a restriction of penetrant diffusivity.[188] Diffusion of the molecules through certain composites depends on several factors, such as void content, penetrant size, segmental motion of the polymeric matrix, degree of cross-linking, of the filler and matrix polarity, and tortuosity of the penetrant path.[189]

6.4. Crystallinity measurement

The crystallinity is usually investigated using X-ray diffraction (XRD), based on Bragg's law, which states that, the X-ray beam scatters when it strikes the parallel planes in a crystal where all atoms can act as scattering centres. The intensity of the scattered radiation can be plotted as peaks in a graph. XRD is used to measure the distance between the crystal planes, crystal orientation, atomic arrangement, size and shape of the crystal, grain size, and degree of crystallinity. Bragg's law can be represented as follows (Eq.1):

$$n\lambda = 2d\sin\alpha \tag{1}$$

where n is an integer, λ is the wavelength of the X-ray, d is the interplane distance, α is the diffraction angle.[190] One of the key elements affecting the physical, chemical, and mechanical properties of cellulose is the presence of crystallinity. The crystallinity index (CrI) is a measure often used to determine the proportion of crystalline cellulose present in cellulosic materials. It was also used to evaluate changes in cellulose structures after physicochemical and biological treatments. X-ray diffraction is now the most commonly used technique employed to calculate CrI. Based on the XRD data, three techniques can be mentioned that are frequently used to determine the CrI of cellulose.[191] The most commonly used and simplest method employed to calculate CrI was developed by Segal *et al*.[192] This method proposes that there are two cellulosic components — crystalline and amorphous, where the amount of the amorphous material is represented by the height of the lowest intensity between the main peaks, while the amount of crystalline material is represented by the height of the highest diffraction peak. The difference between these two intensities, divided by the intensity of the highest peak, is the CrI. However, the peak height calculation introduces a clear error into the accurate measurement of CrI, since the precise quantity of crystalline fraction relates to the peak area rather than to its height. Additionally, a recent study performed by French and Santiago Cintrón.[193] demonstrated that for materials with the same proportion of crystalline cellulose, the CrI determined using this approach depends on crystallite size and cellulose polymorph. Recent research showed how to determine the crystallinity of cellulose with high accuracy, while careful correction for a variety of variables, such as preferred orientation, incoherent scattering, and moisture. The absolute proportion of crystalline material was determined from the peak area with the overall corrected integrated intensity after using Rietveld fitting to generate integrated peak areas from the X-ray data acquired with a digital area detector. In addition, the peak size is a better indicator of the proportion of a crystalline material than the peak height, which the Segal approach correlates with the degree of crystallinity. The method accuracy is hampered by the challenge of selecting peaks that correctly depict the actual diffraction produced by each fraction.[193, 194] Scherrer's equation (Eq. 2) established a significant correlation between a crystal's size and a particular peak width at half-maximum (pwhm)

$$\tau = \frac{\mathrm{K}\,\lambda}{\beta\cos\theta} \tag{2}$$

where τ is the size perpendicular to the lattice plane, K is a constant that depends on the crystal shape, λ is the wavelength of the incident beam, β is the pwhm in radians and θ is the position of the peak.[195, 196] XRD was extensively used to investigate the change in crystallinity of the NC and its polymer composites and their impact on the different properties of the composite. Ilyas *et al*.[44] used XRD to estimate the crystallinity of the prepared CNCs from sugar palm fibers (*Arenga Pinnata*), where it was found that the crystallinity of the extracted CNCs was 85.9% *vs* 55.8% in raw sugar palm fibers. The improvement in crystallinity was attributed to the removal of amorphous compounds, such as amorphous cellulose, hemicellulose, and lignin due to the bleaching, alkali and hydrolysis treatments. Guimarães *et al*.[175] reported that the incorporation of 6.5% of nanofibrils extracted from bamboo pulp increased the crystallinity index of the starch/poly(vinyl alcohol) nanocomposite by $\sim$10% which has a positive effect on improving the tensile properties of the nanocomposite. Khoo *et al*.[197] studied the effect of NC on the thermal stability and

crystallinity of PLA/NC bionanocomposites. It was found that the addition of CNC increased the crystallinity from 30.9% for pure PLA to 34.5%. The thermal stability was also improved.

6.5. Morphological properties

Three common techniques are used to study the morphology of NC and its polymer composites. The first technique is atomic force microscopy (AFM), in which the surface characteristics of the cellulose filler suspension or its composite are investigated. Scanning electron microscopy (SEM) is the second technique that is always used to measure the particle size of the dispersed fillers and their distribution in the matrix. The micrographs of the composites are always compared to those of the neat polymer or those that are free from the filler under investigation. Good filler dispersion in the matrix will result in improved the mechanical and other properties. Transmission electron microscopy (TEM) is the third technique that is considered a valuable tool to visualise the size of nanoparticles and their dispersion in the polymer matrix. This method was also used to study the morphology of nanoparticle fillers in the polymeric matrix governing the improved mechanical, thermal, physical, and barrier properties of the nanocomposites. Saba *et al.*[198] investigated the effects of various CNF concentrations (0%, 0.5%, 0.75%, and 1%) on the properties of their epoxy composite. The results showed that there wasn't any aggregation at concentrations of 0.5% and 0.75%, while the aggregates and micro cracks were observed at a concentration of 1% CNF, as indicated by Fig. 11. The aggregation of CNF at a relatively high concentration of CNF (1%) caused a non-uniform distribution of stress in the composite, and consequently, the tensile and impact strength decreased. In TEM analysis, similar results were obtained, where a uniform dispersion of the CNF was observed at a concentration of up to 0.75%, while at 1%, the agglomerated CNF appeared clearly as illustrated in Fig. 12.

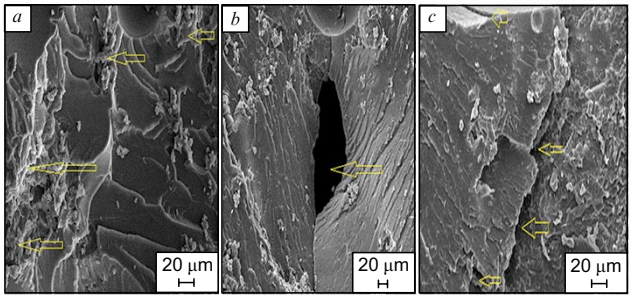

Figure 11. SEM images of Epoxy/1% CNF showing agglomerations (*a*), void (*b*), and deep fracture (*c*).[198] The figure is published with permission by Elsevier.

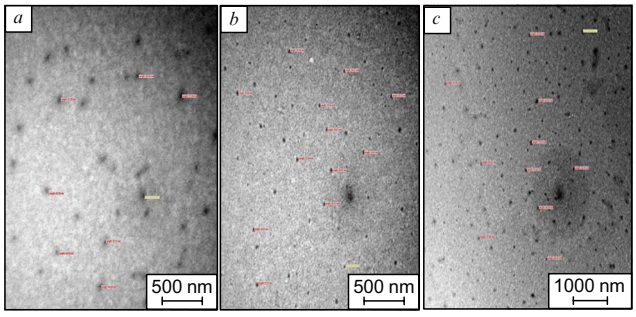

Figure 12. TEM images for 0.5% (*a*), 0.75% (*b*) and 1% (*c*) of CNFs/epoxy nanocomposite.[198] The figure is published with permission by Elsevier.

6.6. Fourier transform infrared spectroscopy (FTIR)

The infrared spectrum of a solid, liquid, or gaseous object can be obtained using this method of characterization. FTIR is frequently used to analyse the molecular group involved in bonding between NC and matrix and surface modification of NC. Tto add functional groups with covalent bonds, processes including oxidation, esterification, carbamation, and amidation are used to modify the NC surface.[199] To ensure that cellulose and NC were successfully isolated from raw sources, FTIR is utilised as a key characterisation tool. The molecule of cellulose has multiple bonds on its surface, including C—C, C—H, C—O—C and OH. Stretching and vibrations of OH bonds present on the NC surface usually appear as a peak between 3200 and 3600 cm^{-1} Stretching of the C—H occurs between 2800 and 2950 cm^{-1} The peak between 1635 and 1650 cm^{-1} indicates the presence of adsorbed water (moisture). The peak at 1034 cm^{-1} is attributed to the C—O—C bond of asymmetric 1,4-glycosidic linkages of d-glucose. The C—H and C—O vibrations in the polysaccharide ring of NC causes a peak at $\sim$1250–1390 cm^{-1} (Ref. 200) Mandal and Chakrabarty[201] used FTIR to analyse the functional groups that characterize polyacrylamide (AAm), PVA and NC extracted from sugarcane. The characteristic peaks of the primary amide NH bond and C—OH stretching vibrations of PVA appeared at 3185 and 3250 cm^{-1} A broad band at 3400 cm^{-1} was attributed to O—H stretching vibration of NC.[201] Dai *et al.*[126] observed an increase in the peak intensity for O—H groups resulting from the increased hydrogen bond interactions between gellan gum and NC extracted from pineapple peel. Kardam *et al.*[202] observed that the intensity of the characteristic peaks of lignin decreased after alkali treatment which was attributed to partial removal of lignin.[202]

6.7. Raman spectroscopy

Nanocellulose doesn't have characteristic Raman spectra, therefore, this technique can not be used to confirm the presence of NC. However, there is a difference between different types and sizes of cellulose such as CNF and CNC, in Raman frequency, shape, and band intensity. In most cases, the highest intensities of Raman spectra bands are recorded for highly crystalline CNC. Based on the rate of a particular Raman band shift due to strain or stress, Raman spectroscopy can be used to investigate the stress transfer between NC and polymeric matrix and interfacial tension. Bulota *et al.*[203] studied the stress transfer from polymeric matrix to NC in PLA/TEMPO-oxidized fibrillated cellulose (TOFC) composite. The Raman spectra was recorded during tension of microtensile specimens to investigate the deformation micromechanics. The shift of the Raman peak at 1095 nm, assigned to C—O—C stretching in the cellulose structure, was monitored during deformation as an indicator of stress transfer from the matrix to the filler. The highest shift was observed for the more acetylated TOFC filler. Rusli *et al.*[204] studied the effect of the orientation of CNC nanocrystal on the stress transfer from polyvinyl acetate (PVAc) matrix to a CNC filler. The peak at

1095 cm^{-1} in the Raman spectrum was shifted as a result of uniaxial deformation in the PVAc/CNC nanocomposite. This shift was used to determine the degrees of stress experienced by the CNCs, not only *via* stress transfer from matrix to CNC but also between CNCs molecules. Tanpichai *et al.*[205] used Raman spectroscopy to monitor the deformation occured in the CMF/PLA composite during tension. The tensile strength and elastic modulus were improved after addition of CMF by 14% and 60%, respectively, in comparison with those for neat PLA. It was found that the Raman band at 1095 cm^{-1} was shifted to lower wavenumbers upon deformation while the rate of this shift was higher for the composite than for the neat CMF, indicating that the improvement in mechanical properties is due to stress transfer from PLA matrix to CMF. The Raman spectroscopy was used to investigate the interaction between NC and poly(butylene adipate-co-terephthalate) (PBAT) matrix. With an increase in the NC content, the shift in Raman spectroscopy peak at 1095 cm^{-1} increased, indicating greater interaction between NC and PBAT *via* hydrogen bonding, which lead to an increase in mechanical properties.[206]

6.8. Biodegradability

The versatility in the applications of petroleum-based synthetic polymers, along with their resistance to biodegradation, will lead to their accumulation in large quantities. This will eventually cause a serious environmental problem at the global level. In addition, the release of carbon monoxide arising from the incineration of non-biodegradable polymers will increase the deepening threat of global warming.[5,207] Biodegradable plastic is a good alternative solution to this issue because it is less environmentally harmful and doesn't contribute to the accumulation of solid waste upon disposal. The incorporation of biodegradable cellulosic filler imparts partial biodegradation to non-biodegradable petroleum-based polymeric composites, while for biodegradable polymers, it will produce a completely biodegradable composite. The biodegradability of plastics depends on the starting raw materials and the chemical composition and backbone structure of the polymeric materials, as well as on the environment where they are expected to be disposed. Biodegradation involves many steps that can be summarised as follows: 1) adherence of the microorganism to the surface of the material, forming a biofilm; 2) growth of the microorganism utilising the degraded polymer as a food and energy source; 3) fragmentation of the polymer (degradation); 4) polymer disintegration. Microbes can degrade the polymeric materials through aerobic or anaerobic oxidation. In aerobic oxidation, the biodegradation products are carbon dioxide and water, while in anaerobic oxidation, which is carried out in the absence of oxygen, the products include carbon dioxide, water, methane, hydrogen sulfide and ammonia. Many microorganisms can cause biodegradation of synthetic and natural polymers, such as fungi and microbes. The biodegradation environment significantly affects the rate of biodegradation, where the habitat of microorganisms varies among soils, activated sludge, water and compost.[208] For high-molecular-weight polymers, enzymatic biodegradation is more effective, where the enzyme converts them to lower-molecular-weight polymers available for further microbial degradation.[209] Platnieks *et al.*[171] investigated the effect of the addition of 40% NC in the form of CNF and MCC in various ratios on the biodegradation rate of biodegradable poly(butylene succinate) (PBS). The biodegration was carried out using a soil burial test (composting conditions). The addition of CNF/MCC accelerated the decomposition rate from 75 days to 60 days.

6.9. Biocompatibility and cytotoxicity

Biocompatibility is defined as the ability of foreign body material to perform the required action and remain in harmony without causing a subtle adverse response to the host.[210] The biocompatibility of polymers and biocomposites based thereon for biomedical applications depends on many parameters such as morphological form and fabrication method of nanomaterials and also the copolymer amounts, chemical structure and active groups of the polymer.[211] that affect cellular activity test. The NC and its based biocomposites cytotoxicity is still in the early stages of research and its main adverse effects are not yet clear to provide a safer by-design approach. In general, low uptake of NC is usually used, that does not reach a level producing a remarkable impact or causing detrimental effects on the cellular and genetic levels, as well as in organ and in animal *in vivo* tests. Unfortunately, the self-aggregation of NC results in difficult degradation in the animal's body and might cause pulmonary inflammation especially if inhaling a large amount of it (particularly CNC).[212] As a result, surface modification of chemical groups on NC significantly reduced the proinflammatory response.[213] Also, the use of NC and its biocomposites is still desirable because of their relatively low cytotoxicity compared to other materials. The biocompatibility and toxicological properties of NC and its nanocomposites for biomedical applications have been reviewed in great detail by Stoudmann, *et al.*[214] and Ventura, *et al.*[215] Table 6 represents various analysis techniques used to characterise the NC polymer composites in the previous state of the art.

7. Applications

Nanocellulose polymer composites are used in a many fields. In particular, they found application in the paper and packaging industries. Furthermore, due to the nano-sized cellulose filler, high strength and stiffness, cellulose-based nanocomposites are of interest for their potential uses in a variety of industries, including construction (structural composites), automotive (for manufacturing parts based on micropatterns), electronics (membrane for electroacoustic devices), pharmacy (biomedical applications), and cosmetics. Nanocellulose composites can also be used as membranes for ultrafiltration, ion exchange, and fuel cells.

7.1. Sensor

The sensor should be easy-to-manufacture, cheap, and have high sensitivity, selectivity, and rapid detection of analytes. Nanocellulose is readily available, biocompatible, and highly versatile material compatible with many molecules and having a lot of functional groups. All these factors make NCs attractive for sensing applications. They are always used in combination with other components in the fabrication of sensors. Weishaupt *et al.*[217] developed a sensor for copper ions (Cu^{2+}) based on cyanobacterial C-phycocyanin/CNF. This sensor is capable of detecting Cu^{2+} ions at concentrations of up to 0.2×10^{-6} M. Bromopyrene/CNC composite was used as a sensor for Fe^{3} ions at minimum and maximum detection limits of 1×10^{-6} and $5000-10^{-6}$ mol., respectively.[218] The theory of electro-

Table 6. Techniques used to characterize various NC polymer composites.

Nanocellulose polymer composite	Characterization technique	Composite features	Ref.
Polypropylene (PP)/CNC	Flammability test, dynamic mechanical analysis (DMA), TGA, and TEM	The CNC was extracted *via* acid hydrolysis of the bleached and unbleached kenaf core chips. The unbleached CNC-containing composite showed higher thermal stability and higher thermo-mechanical properties than that containing bleached CNC. The flammability rate of unbleached CNC nanocomposites was 28.79 *vs* 15.95 m s^{-1} for bleached CNC nanocomposites	216
Epoxy/CNF	Tensile test, impact test and flexural test, TGA, and SEM, TEM, Elemental dispersive X-ray analysis (EDX), FTIR, and XRD	The CNF was added to epoxy at different loadings (0.5%, 0.75%, 1% by wt.). The best distribution and, consequently, better mechanical properties were recorded for 0.75% of CNF. XRD patterns showed no considerable change in the crystallinity of the epoxy matrix	198
PBS/MCC/CNF	TGA, DSC, DMA, tensile test, contact angle, SEM and biodegradation	The storage modulus increased significantly after addition of MCC and CNF. The addition of cellulosic filler accelerated the biodegradation of PBS composite, with the composites disintegrating 10 days faster than the pristine PBS	171
Natural rubber (latex)/MCC and/or CNC	FTIR, XRD, swelling in toluene, SEM, and TEM	The XRD analysis showed that CrI of the extracted CNC increased to 92.95%. SEM and TEM analysis showed that the shape of these CNCs was rod-like or whiskered and the dimensions of the CNCs were approximately $130.02 \pm 48.55 \times 5.14 \pm 2.03$ nm (length × width). The CNC was added at different loadings (0, 2.5, 5, 7.5, and 10 phr), where the best distribution of CNC and the highest mechanical were observed for 0.25 phr	173
Epoxy resin/CNC	Zeta potential, TEM, FTIR, DSC, TGA, DMA, and tensile test	Compared to neat epoxy, at 15 wt.% CNC, the storage modulus increased by 100%, the Tg increased from 66.5 to 75.5 °C, and tensile strength increased from 40 to 60 MPa	174
Polyvinyl alcohol/starch/CNF	AFM, DSC, XRD, FTIR, tensile test, SEM, density, and water absorption	DSC analysis showed a significant rise in the values of the CNF reinforced nanocomposites' melting points (6%), melting enthalpy (23%) and crystallisation enthalpy (55%). CrI, tensile strength, tensile modulus, and elongation at break also improved for composite compared to the original composite	175
PHA and PLA with CNC or MFC [a]	AFM, SEM, TEM, contact angle, UV – visible spectrophotometer, FTIR, and tensile test	CNC was added at of 1, 2 and 3% loadings for PHA and PLA, while MFC was added at of 10, 20, and 30% loadings. CNC showed higher reinforcing action than MFC with both polymers, where the CNC-containing composites demonstrated higher tensile strength than that containing MFC. The addition of CNC preserves the thermal stability of the PLA films while the MFC decreased it, and both MFC and CNC the thermal stability of PHA	177
Polyhydroxybutyrate(PHB)/ CNF or CNC	SEM, XRD, TEM, AFM, UV – visible spectrophotometer, barrier performance test, TGA, DSC, and tensile test	CNF improved the thermal stability of PHB more than CNC. The transmittance of the composite film decreased with the increase of the CNF and CNC content. The water vapour and oxygen transmission rates of PHB were significantly reduced after the addition of NC	178

[a] MFC is microfibrillated cellulose.

chemical sensors depends on the gas reaction and production of electrical signals proportional to the gas concentration.[219] The main components of electrochemical sensors are the sensing electrode and the counter electrode separated by thin layer of electrolyte.[220] When the gas passes through the sensor capillary tracks, the interaction takes place and spreads in the barrier matrix untill it reaches the electrode surface. This allows the flow of gas in a sufficient amount for the production of an electrical signal without any leakage.[221] For sensors of gases including those water-soluble like H_2S, NH_3, CO_2 and CO, CNF and its composites can be hybridized with conducting materials as a host substrate. CNF can be used as alternative green material in the sensor industry. Shahi *et al.*[222] extracted CNF and oxidized cellulose nanofibers by TEMPO (TOCNF) from rice husks (Fig. 13) prepared CNF, TOCNF, and TOCNF with glycerol (TOCNF/G) dispersions on a polyimide substrate and found that CNF, TOCNF and TOCNF/G manifested high sensitivity for several gases especially for acetone and ammonia under ambient conditions. The graphene oxide (GO)/CNF nanocomposite prepared by grafting CNF on functionalized GO showed remarkable sensitivity to various organic solvents (toluene, choloroform, n-hexan, acetone and ethanol) based on the diffusion

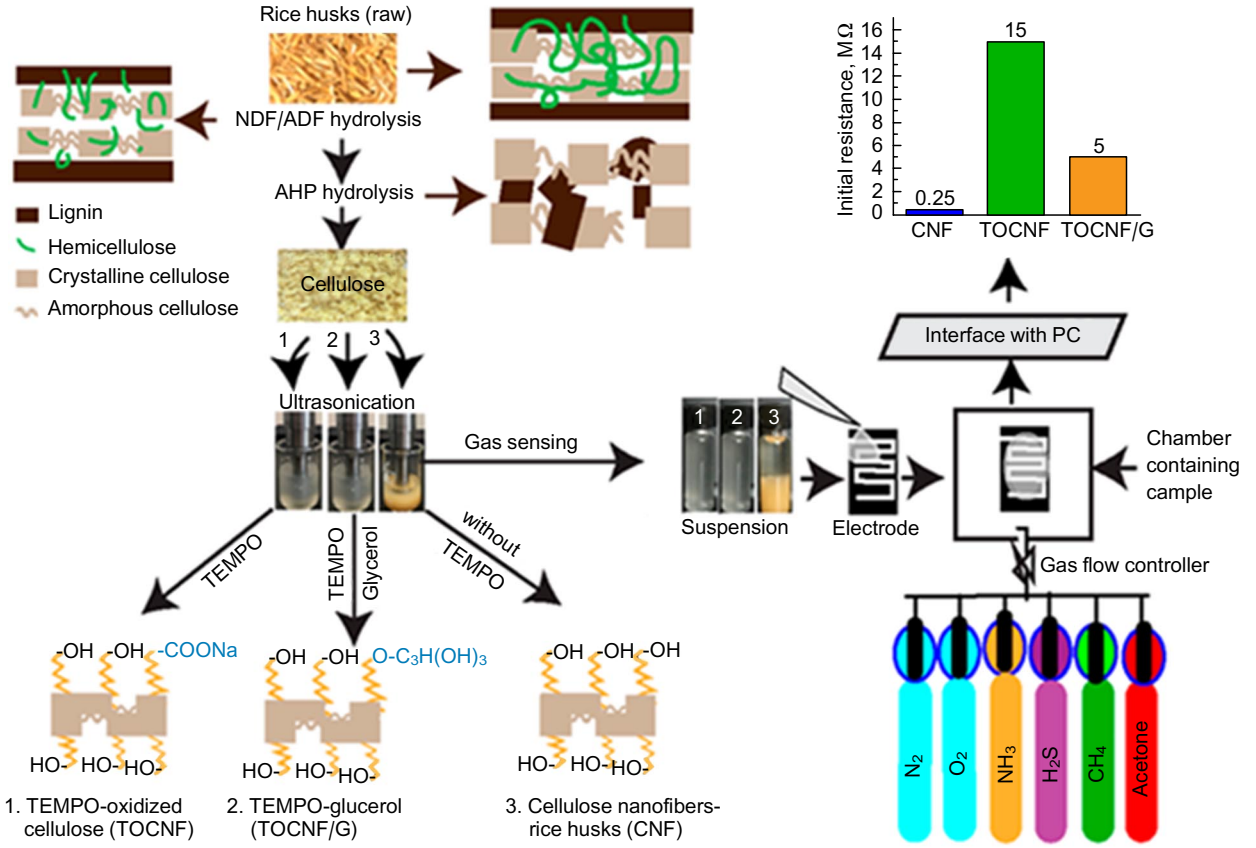

Figure 13. Application of CNF and modified CNF in sensors for various gases.[222] Published in accordance with the Creative Commons Attribution license CC BY 4.0.

mechanism.[223] The CNF with reduced GO nanosheets were prepared as temperature sensor and detected tunnelling frequency values of 1×10^{-7}, 2.8×10^{-7}, 8.8×10^{-7} and 1.5×10^{-6} at a temperature of 25, 40, 60 and 80 °C. The sensor fabrication method was based on partial thermal reduction of GO that is necessary for electrons motion inside the CNF matrix.[224] Han *et al.*[225] synthesized the electroconductive CNF-polyaniline/natural rubber elastomers and showed that the elastomers exhibit excellent mechanical properties, flexibility, and conductivity up to 8.95×10^{-1} S m^{-1} suggesting these elastomers could be applicable as human activity monitoring sensors.

7.2. Electronics industry

Nanocellulose composites can be used in the electronics industry due to their enhanced flexibility and conductivity. Numerous methodologies have been used to modify both CNF and CNC to provide the nanomaterials with additional functions and thereby broaden their range of applications. A viable strategy for the development of next-generation flexible electronics is to combine many components, each performing a specialized function, and integrating them into a single device. Liu *et al.*[226] studied the use of polyaniline and NC composites as a conducting film. The thin composite film displayed good flexibility and conductivity. The conductivity value of the composite film containing 30 wt.% of polyaniline, reached 1.9×10^{-2} S cm^{-1}, which makes it possible to use it as a flexible electrode, paper-based sensors, and conducting adhesives. Polyaniline and NC composite was used as electrodes for high performance flexible supercapacitors,[227] and for electrochromic devices.[228] It was reported that the flexible CNF, reduced graphene oxide (rGO) and polypyrrole aerogel electrodes achieved favorable electrochemical characteristics with a maximum energy density of 60.4 μW h cm^{-2} under different bending conditions, and could be promising in the field of flexible electronic devices industry.[229] Yang *et al.*[230] fabricated the CNF substrate by applying the TEMPO-oxidized wood fibers (TEMPOWF) on the top surface of CNF films. It was found that when the amount of TEMPOWF and roughness of the upper surface increased, the smoothness decreased and consequently, the optical transparency of films was reduced. The authors reported that the transparent films with optical haze ranging from 3.8% to 62.3% are required for the next steps in green technology in optoelectronic devices. Supercapacitors have higher energy performance, longer life cycle, they are safer and environmentally less harmful compared to batteries.[219,231] Fukuhara *et al.*[232] fabricated an amorphous NC fiber supercapacitors and showed that these devices could provide high-performance electric energy storage of about 221 mJ m^{-2}, 13.1 W kg^{-1} The authors reported that CNF are an ideal substrate for supercapacitors to be applied in light electricity such as transportation, handheld electronic devices, and renewable energy storage for power grids. NC presents dielectric matrices due to its excellent dielectric constant, extreme transparency, perfect mechanical properties, light weight and low thermal expansion coefficient. The most commonly used fillers for NC-based high dielectrics are $BaNO_3$,[233] TiO_2 (Ref. 234) as ceramic

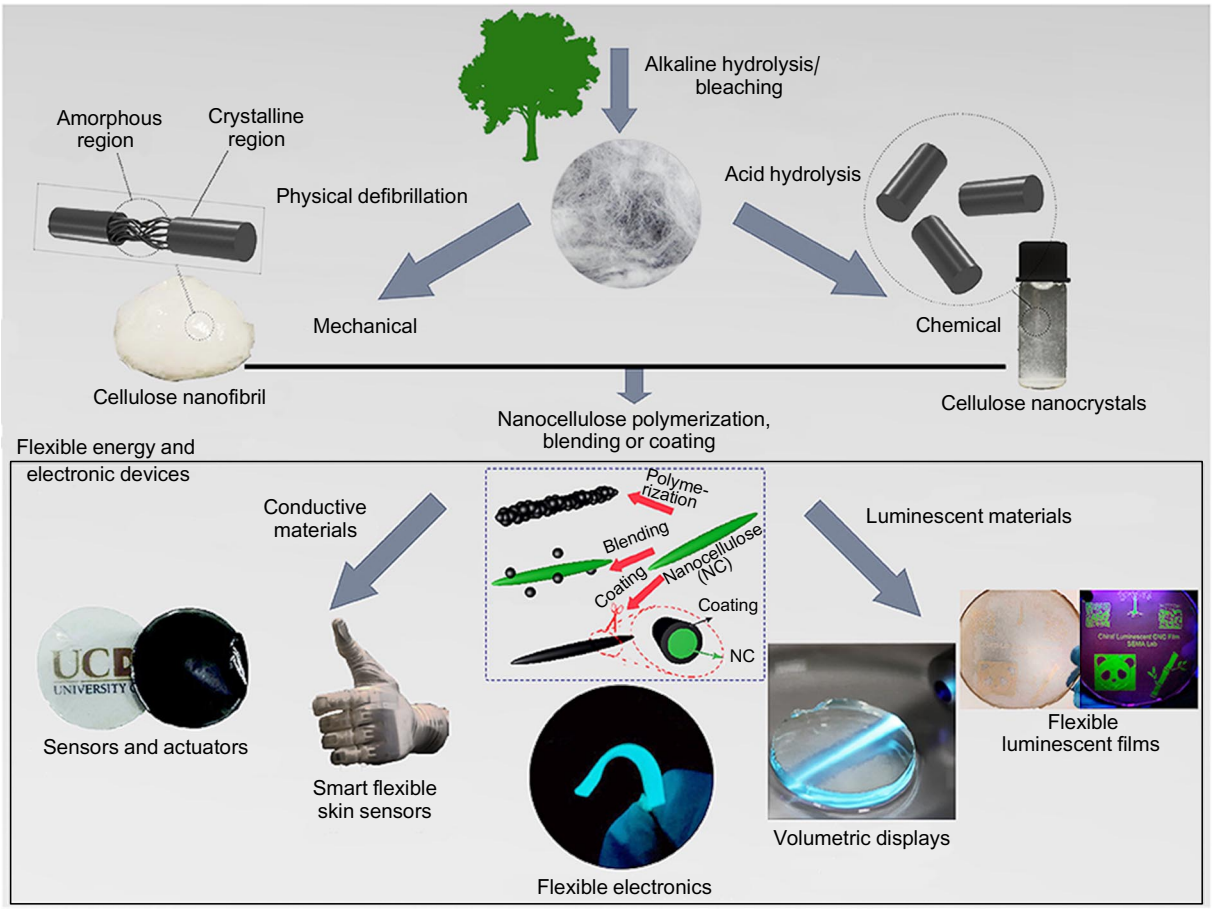

Figure 14. Surface functionalization of CNC and CNF for application in flexible energy and electronic materials.[242] Published in accordance with the Creative Commons Attribution license CC BY 4.0.

fillers and silver nanowires (AgNW),[235] graphene oxide (GO),[223, 236, 237] triglycine sulfate (TGS),[238] polyaniline (PANI),[239] carbon nanotubes (CNTs)[240] as conductive fillers. Tao and Cao[241] fabricated flexible high dielectric composite films from CNF and acid-oxidized multi-walled carbon nanotubes. The resulting composite films showed high dielectric, flexibility, and mechanical properties to be potentially utilized in the energy storage system. Figure 14 shows the ways of using CNF and CNC in production of new hybrid electronics.

7.3. Fuel cells

The proton exchange membrane is the main component in fuel cells, and thus it can influence the performance, cost, and potential application of the cell. CNF was impregnated in different concentrations of phosphoric acid solution and embedded into sulfonated polyether sulfone to develop a proton exchange membrane. The membrane displayed improved proton conductivity, water uptake, and methanol resistance. The addition of the phosphoric acid-doped CNF generates proton transport sites[243] Xu *et al.*[244] embedded CNF in sulfonated poly (ether sulfone) to increase the water retention and to improve the proton exchange of proton exchange membranes. The hydrophilicity and, consequently, the water uptake were improved after the addition of CNF. Bayer *et al.*[245] studied CNC and CNF membranes for fuel cell applications. CNF and CNC papers were fabricated and recorded high proton conductivity (a maximum conductivity of 0.05 mS cm^{-1} at 100 °C for CNF and of 4.6 mS cm^{-1} at 120 °C for CNC) that were dependent on humidity, temperature and the type of NC. The authors showed that the higher conductivity of CNC membrane resulted from the increase in the number of charge carriers and the sulfuric acid groups of H_2SO_4 introduced through the hydrolysis process. The authors prepared two fuel cells using two CNCs and CNF papers and found that CNC papers showed superior performance of (17 mW cm^{-2}) compared with CNF (0.8 mW cm^{-2}). Sriruangrungkamol *et al.*[246] prepared a solid electrolyte membrane for methanol fuel cell application using vacuum filtration of CNF suspension isolated from Para rubber wood sawdust. The membrane was treated with sulfosuccinic acid and activated in hot press at 120 °C for 1 h. Ion exchange capacities (IEC) of unmodified and modified NC membrane ranged from 0.005 to 0.069 mmol g^{-1}, while the water uptake ranged from 28% to 61%. The modified NC membrane exhibited better methanol barrier property and proton conductivity than the neat NC. Priyangga *et al.*[247] prepared NC based membrane for direct methanol fuel cell. The NC membrane was mixed with 2 wt.% phosphotungstic acid (PTA) and 5 wt.% imidazole (Im). The highest proton conductivity was recorded for NC/Im membrane (14.98 mS cm^{-1}) while NC/PTA, NC/Im/PTA, and neat NC membrane showed 13.17, 6.34, and 5.32 mS cm^{-1}, respectively. In addition, the highest selectivity (2.00×10^4 S s cm^{-3}) was recorded for NC/Im membrane. A membrane based on a blend of

BNC and lignosulfonates (LS) and tannic acid as crosslinker, was fabricated for polymer electrolyte fuel cells. The fabricated membrane recorded maximum moisture-uptake capacity of 78% after 48 h. The membrane with highest percentage of LS showed maximum ionic conductivity of 23 mS cm^{-1} at 94 °C and 98% RH with good mechanical and thermal stability.[248] Ternary materials including mesoporous phosphotungstic acid (m-PTA), imidazole (Im), and NC were fabricated using a phase inversion technique. The fabricated membrane exhibited proton conductivity, membrane selectivity, and methanol permeability at 31.88 mS cm^{-1}, 1.83×10^4 S s cm^{-3}, and 1.74×10^{-6} cm^2 s^{-1}, respectively.[249]

7.4. Construction

Due to the high strength and stiffness, NC based composites can be used in load-bearing walls, roof systems, staircases, and subflooring or as biofoam in insulation. The applicability of biobased composite materials in roof structures has been investigated. Structural beams were developed, fabricated, and tested, giving promising results. In addition, cellulose nanomaterial can form thin transparent films, and so, they can replace glass and plastic for windows and screens, or as an additional layer for UV or IR barriers. The addition of cellulose nanomaterial to cement mixes can enhance the hydration process, change the rheology, and improve flexural strength. The mechanical properties and fracture characteristics of concrete can be enhanced with cellulose nanomaterials by arresting micro-cracks formed during hydration and preventing their further growth.[250] The addition of TEMPOCNF into the cement enhanced the flow control of fresh cement paste and also played as curing agent resulting in lower crack and shrinkage growth in the formed concrete. Fire protection and thermal insulation are considered the most critical characteristics affecting safety and energy efficiency in built environments.[251] The biofoam composed of CNC, PVA and a crosslinking agent (mass ratio: 74, 7.5 and 18.5 wt.%, respectively) was fabricated in water. The formed foam showed a stress of 73 kPa at 50% strain and an elastic strain of 13% at a modulus of 250 kPa, that was 18 and 100 times, respectively, higher than those of pure CNC foam. The foam not only manifested higher thermal conductivity of 0.027 W m^{-1} K^{-1} compared to those of traditional insulating materials but also the structural integrity kept unchanged after burning. The authors recommended the use of CNC-based materials in high-performance insulation applications.[252] Tannin rigid foams were suggested as practical and continuous alternatives for traditionally used in frame buildings. Missio *et al.*[253] synthesized tannin foams from the ester copolymerization of unpurified black wattle tannin, furfuryl alcohol and CNF. The authors showed that the CNF acted as both reinforcing agent and crosslinking agent. The foam formed by addition of 0.1% of CNF was a highly entangled and interconnected network that was stronger and lighter by ~30 and ~25%, respectively, relative to those produced with benchmark formaldehyde crosslinker. The foam formed in the presence of CNF showed higher thermal degradation temperature shifted from 30 °C to 50 °C and fire resistance with 40% decrease in mass loss compared to those formed by formaldehyde crossliking.

7.5. Paper and board

Cellulose nanocomposite has potential applications in the paper and cardboard industries, where it can be used as a strengthening agent. Cellulose nanocomposite can increase the bond strength between cellulosic fibers and thus increase the mechanical properties of these materials. Burst strength, smoothness, density, and barrier properties of paper and cardboard can also be improved by the incorporation of nanocomposites. The Polyhexamethylene guanidine/NC composite was used to improve the folding strength of ancient paper by 1.78 times.[254] Waterproof paper with antibacterial properties was prepared by dip coating of silver nanowires AgNWs / CNC / beeswax composite on the cellulose paper. The modified papers gained an efficient electromagnetic interference shielding (up to 46 dB) and adorable mechanical flexibility. The modified paper still kept its high waterproofness even after dozens of bending tests or 1.000 peeling tests. The modified paper could be promising for packaging conductive components and electromagnetic interference shielding elements applications, even under extreme conditions[255] Barbash and Yashchenko[256] prepared NC from non-wood plant raw materials (wheat straw, kenaf and flax fibers),and found that the low amount of NC is able to enhance the physico-mechanical features of paper and cardboard and meet the requirements recommended for paper industry application. Also, Perdoch *et al.*[257] studied the coating effect of CNC, CNF and carboxy CNF on physico-mechanical properties of paper substrate and found the significant increase in the strength of paper enriched with functionalized NC (containing carboxyl groups). Pego *et al.*[258] used NC to improve the different physical and chemical properties of paper manufactured from blend of cellulosic fibers (eucalyptus, sisal, and pine). The NC was added either through with mixing with pulp (3%, 5%, and 10% NC) or through coating of dry paper (superficial coating with 10% NC). Regardless of the mixing technique, the modification by NC increased the physical properties such as thickness, volume, grammage, and opacity. In addition, the mechanical properties including tensile strength and fold endurance, were improved.

7.6. Biomedical applications

Because of its great biocompatibility, low toxicity, self-assembly behaviour, crystallinity, distinctive geometry, rheology, and surface chemistry, NC and its composites are a remarkable biomaterial for medical applications. It was found that CNCs have an antimicrobial effect, high water holding ability, and excellent mechanical properties, which allows them and their composites to be used in wound healing dressing. Generally, biomedical applications can be divided into several categories, such as pharmaceutical applications (*e.g.*, drug delivery), general surgical applications (*e.g.*, skin substitutes and burn dressings), dental applications (*e.g.*, implants, scaffolds), ophthalmologic applications (*e.g.*, retinal prostheses and contact lenses), and biosensors. Several research articles on NC polymer composites for biomedical applications have been published. Tang *et al.*[259] used PVA-doped bacterial NC tubes in the manufacturing of artificial blood vessels. The results showed that the composite prepared from BNC and PVA exhibited improved mechanical properties and water permeability, which enabled the produced composite to act as a new biomaterial for vascular grafts. To avoid the potential immunogenicity and toxicity, crystal NC grafted with polyethyleneimine was used as an alternative material to traditional viral vectors.[260] Carvalho *et al.*[261] fabricated composite patches based on BNC, hyaluronic acid (HA)

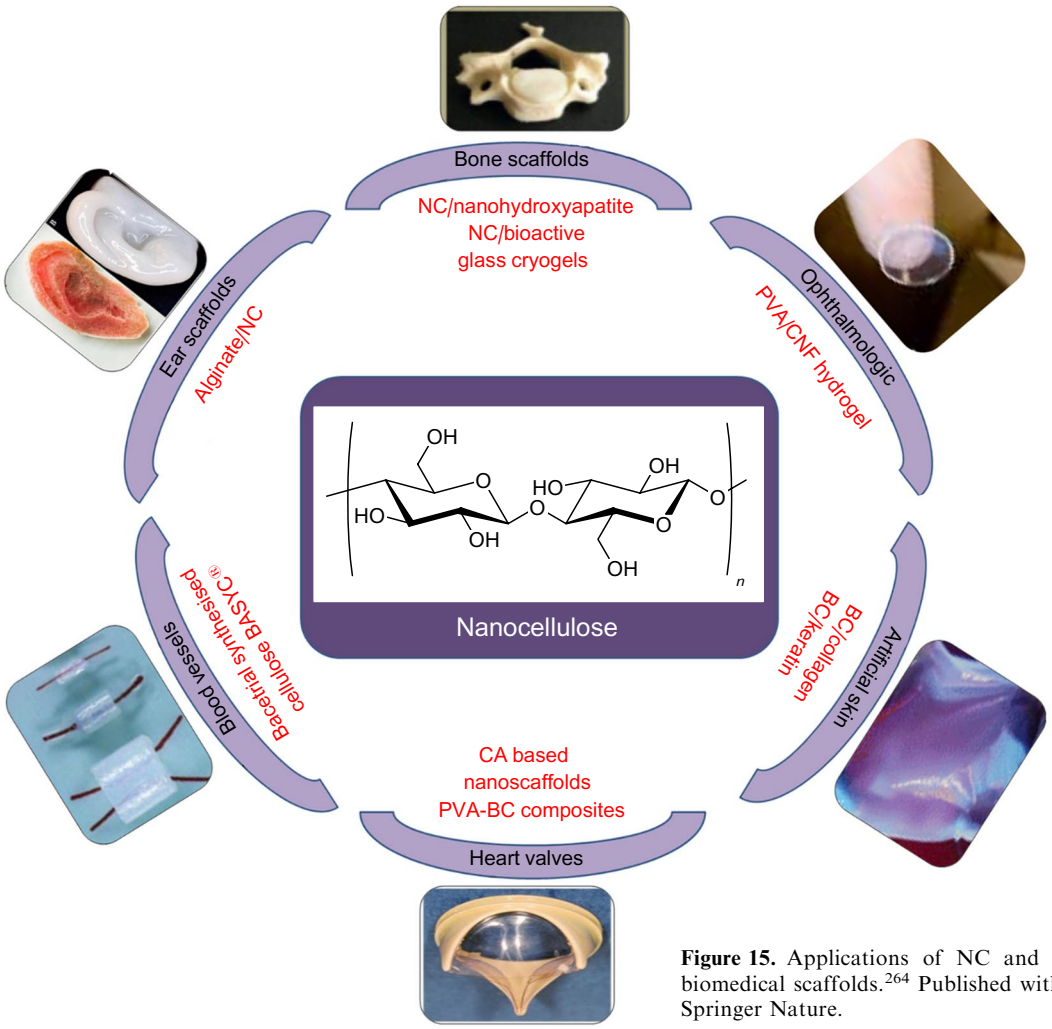

Figure 15. Applications of NC and its composites as biomedical scaffolds.[264] Published with permission from Springer Nature.

and diclofenac (DCF) for the treatment of aphthous stomatitis. The release of DCF from the composite patches in simulated salivary fluid showed that these composites could be promising for alleviating discomfort of aphthous stomatitis. Ghafari *et al.*[262] developed a bilayer scaffold that can be applied in tissue engineering of skin. The scaffold was composed of CNF and PVA composites (Dermis: 1.4 wt.% CNF, 0.35 wt.% PVA and Epidermis: 1.4 wt.% CNF, 0.35 wt.% PVA). The authors found that the interconnected porous structure of these scaffolds had a definite size similar to each dermis and epidermis layer (two primary human skin layers), and the cross-linking formed by intra-/inter-molecular hydrogen bonding between the hydroxyl groups of CNFs/PVA provided an effect of the weak mechanical properties of scaffolds. The fabrication of multilayer thin films as drug carriers using CNC (anionic polymer) and chitosan (cationic polymer) by layer-by-layer technique was investigated with loading doxorubicin hydrochloride (hydrophilic drug), and a curcumin (hydrophobic drug) as anticancer drugs. It was found that CNC interacted with curcumin and doxorubicin through the hydrogen bonding and van der Waals interactions to produce stable dispersions in water. The release profiles of curcumin and doxorubicin conjugates achieved steady state in PBS buffer with pH 7.4, while doxorubicin release was higher in acidic pH of 6.4.[221] Sarkar *et al.*[263] fabricated composites of CNF/chitosan as transdermal films. The authors reported that the mechanical strength of CNF/chitosan films was improved and the drug release rate decreased with increasing the CNF concentration. The release profile of drug within 10 h was 40% when the amount of CNF in the formulation became 1 wt.%. The authors recommended CNF/chitosan films as a potential architecture for transdermal drug delivery systems. Nanocellulose was also used in numerous biomedical applications, including the production of cosmetic tissues, animal wound dressings, artificial blood vessels, and nerve surgical cuffs. Figure 15 shows several biomedical implants made from NC and its composites.

7.7. Food packaging

Increasing population means the need for more food. A report by the Centres for Disease Control and Prevention estimates that more than 70 million people suffer from food-related diseases each year. Food production and safety are thus the most vital requirements. Food must now be packaged properly to avoid tampering, contamination, spills, atmospheric conditions, and for safe transit.[265] Additionally, it reduces food waste and maintains the nutritional content of food. Food safety is greatly influenced by food packaging. Packaging is an external protective layer that protects food from potential physical, chemical, and biological risks. Numerous polymers including natural and synthetic types, that have been investigated and are readily available in the market, play a significant role in the

creation of packaging films. Due to their non-toxic, renewable, and ecologically beneficial qualities, natural biopolymer-based films have increasingly replaced conventional petroleum-based packaging materials. The polymers used in food packaging must be able to isolate gases and water and be somewhat hydrophobic. They should be flexible and strong enough to resist damage caused by heat, chemicals and microorganisms. In addition, it is recommended that they be transparent to allow the food quality control upon storage.[266] Many biopolymers were used as packaging materials such as polyhydroxyalkanoates (PHA), PLA, chitosan/chitin, gelatin, and starch.[265] Because of the NC density, entangled nanoporous network and nanoscale dimensions, it was used by scientists in food packaging application. NC was incorporated into many other biodegradable polymers to improve barrier properties, enhance colouring and dying and increase the mechanical properties. BNC was added to poly(3-hydroxybutyrate-co-3-hydroxyvalerate (PHBV) to improve the barrier properties of the resulting biodegradable composite. Also, BNC was plasticized by impregnation in glycerol or polyethylene glycol and then coated with PHBV and dried at 148 °C. The coated and plasticized BNC enhanced the water vapour permeability (from 0.990 to 0.032 g μm m^{-2} day^{-1} Pa^{-1}) and increased the hydrophobicity (contact angle increased from 10–40° to 80–90°).[267] CNF displayed the ability to capture nisin (antimicrobial peptide) and make it available to act as antimicrobial when coming in contact with various microorganisms. The CNF loaded with nisin was used to improve the antimicrobial properties of different food packaging polymers, namely, polypropylene, polyethylene and PLA through casting of CNF-nisin solution on the polymer film.[268] Various NCs, including CNF, CNC and BNC were combined with alginate and chitosan for food packaging application. The results showed that the addition of NC improved the barrier and mechanical properties, where the best results were observed for composites containing CNC.[269] Spherical NC formats (SCNFs) were used to prepare 'green' composite with PLA for food packaging application. Addition of 10% SCNFs improved the tensile strength and Young modulus by 130% and 110%, respectively. In addition, the initial and maximum degradation temperatures increased by 17.4 and 21.5 °C. Moreover, the barrier and migration properties were improved.[270] The addition of 25% CNC to hemicellulose/pectin composite reduced the solubility of the composite film in the fatty food simulant, and hence increased its potential application as a food packaging material.[271] Heidarbeigi *et al.*[272] mixed CNC in varying ratio (0.5%, 1%, 2% and 5%) with low density polyethylene (LDPE) using a melt mixing technique. Due to the incompatibility between polar CNC and non-polar LDPE, the addition of CNC decreases the mechanical properties and increases the gas permeability.

7.8. Water purification

The demand for purified water is growing every day. Many practical technologies, such as membrane filtration, adsorbents, *etc.*, have been shown to be more effective and less expensive than traditional industrial processes. A promising candidate for water treatment application is NC because it is a biodegradable, nontoxic, and sustainable nanofiller with outstanding mechanical properties, a high aspect ratio, a large surface area, and, most importantly, its chemically tunable surface. Many pollutants may present in water such as heavy metals, oils, salts, toxic dyes and microorganisms. Nanocellulose was used as such or as part of a composite to improve the water purification efficiency *via* adsorption or membrane filtration technique. Polyethersulfone- and amine-functionalized cellulose nanocrystals (CNCs) were used for the manufacturing of a membrane for copper ion and direct red 16 azo dye removal from water. The polyethersulfone (PES) membrane embedded with 1% CNCs displayed an adsorption percentage of copper ion and red 16 of about 90% and 99.9%, respectively.[273] Also, a membrane was developed from polydopamine and BNC for wastewater treatment and used to remove a variety of contaminants such as heavy metals (*e.g.*, lead and cadmium), organic dyes (*e.g.*, methylene blue and methyl orange).[274] Polyamide nanofiltration membrane with high permeation flux and good salt rejection was prepared by interfacial polymerization of piperazine. The incorporation of CNC into the membrane composite improved the hydrophilicity of the membrane surface and consequently increased the water flux.[275] A membrane for removal of copper ions and direct red 16 azo dye was based on a composite of PES and amino-functionalized CNC. The modified CNC was added in different concentrations (0, 0.1, 0.5 and 1 wt.%). At 1 wt.% of CNC the membrane achieved the highest removal percentage, which was 90% for copper and 99% for direct red 16 azo dye.[273] Ashori *et al.*[161] investigated the influence of CNC as a nanofiller on the performance of PES membrane at various concentrations (0.1, 0.5, and 1.0 wt.%). The hydrophobicity of the PES membrane increased with an increasing CNC percentage. The highest pure water flux (253 L m^{-2} h^{-1}) was recorded for PES/0.5 CNC membrane compared to 136 L m^{-2} h^{-1} for pure PES. In addition, the CNC improved the removal of bacteria (*Escherichia coli*) where its efficiency reached 62% for PES/0.5 CNC membrane. Zhu *et al.*[276] used CNF template membrane to immobilize Zn-based metal-organic frameworks, zeolitic imidazolate framework-8 (ZIF-8) to degrade organic dye. This membrane provided more than 90% degradation of methylene blue and rhodamine B within 60 min. Shahnaz *et al.*[277] used ethylenediamine tetraacetic acid (EDTA) embedded in CNF for methylene blue removal. The maximum removal percentage was recorded at pH 10, where percentage removal of 98% was achieved for 10 mg L^{-1} concentration of dye.

7.9. Aerogel

Aerogel is a highly porous material produced by a special drying method, and its structure contains a continuous network in which the air represents more than 95%. Due to its high porosity, light weight, ultra-surface area, and low thermal conductivity, aerogel has a variety of applications such as oil absorption, heavy metal removal, electromagnetic shielding, sound absorption and energy storage applications. Due to the environmental issues and shortage of fossil sources, biodegradable and sustainable NC-based aerogels have received a lot of interest in advanced applications.[278] Many drying techniques were used in the preparation of the aerogel, such as supercritical drying, freeze drying, and freeze-casting methods. The supercritical process can effectively maintain and prevent the collapse of the porous structure. This method is expensive and has many complex requirements. Freeze drying is more cost-effective but has a problem with maintaining a porous structure and significant volume shrinkage. The freeze-casting method, also known as ice templating, is a versatile, eco-friendly, extensively used, and simple wet-processing method to

convert the suspension into a porous structure with distinctive and flexible structures.[279] However, the freeze drying method was the most widely used to prepare aerogel for various applications. The CNC was used to improve the layer interaction between the rGO layers using the controllable ice-template technique, which produces a highly stable, flexible, and light aerogel with an excellent layer-stacked structure to act as a carbonized pressure sensor. The prepared aerogel had superior compressibility and super-resilience. This carbonized aerogel exhibited high sensitivity to low strain (0.012%) and small pressure (0.25 Pa).[280] Excellent electromagnetic shielding aerogel was prepared using TEMPO-oxidized CNF, cationic CNC, sodium alginate, and various concentrations (0.22, 0.44, 0.68, 0.89 and 1.2) of carbon nanotubes where the aerogel was formed after freeze drying. The prepared aerogel was conductive, light, had good mechanical properties, and exhibited excellent electromagnetic shielding efficiency.[281] Rafieian *et al.*[282] prepared aerogels *via* freeze drying CNF dispersions with different concentrations of CNF (0.6, 0.9, and 1.2 wt.%). The CNF was modified by hexadecyltrimethoxysilan *via* chemical vapor deposition. The modified CNF aerogel was used to remove motor and cooking oils. All modified aerogels demonstrated a contact angle >90 °C and were classified as hydrophobic. The maximum adsorption capacity was 0.6 wt.% achieving 79 and 162 g g^{-1} for motor and cooking oils. Nguyen *et al.*[283] prepared the GO/CNF aerogel using a freeze-drying technique for methylene blue (MB) removal. CNF was prepared by ultrasonication of alkali-treated and bleached cellulose isolated from petioles of the nipa palm tree. The resulting GO/CNF aerogel had a porosity of more than 98.2% and a light density of 0.0264 g cm^{-3}. It demonstrated more than 99% of MB removal rate in less than 20 min. Mo *et al.*[284] prepared CNF/polyacrylamide aerogel through chemical cross-linking followed by freeze-drying. The prepared aerogel displayed superior water stability, good thermal stability, with a maximum adsorption capacity for Cu(II) ions up to 240 mg g^{-1}. It showed outstanding recyclability where the removal efficiency exceeded 80% after 10 cycles of adsorption/regeneration cycles. Kim *et al.*[285] prepared carboxymethyl cellulose nanofibrils and modified them with polyethyleneimine to produce cationized NC. The resulting material had a high Cr(VI) removal capacity of 1302.3 mg g^{-1} and a high reuse efficiency. Sharma *et al.*[286] prepared an aerogel based on dialdehyde CNC, nanobentonite and carboxymethyl chitosan. This aerogel demonstrated an extraordinary ability to adsorb various contaminants, including oils, dyes and organic solvents. It recorded maximum adsorption capacity of 29.84 g g^{-1} and 20.93 g g^{-1} for Bromophenol blue and Direct Blue 6, respectively, and up to 50 times of its own weight in case of oil and organic solvents (Fig. 16).

7.10. Hydrogel

Hydrogel was discovered in 1960 and has gained a great interest in the last two decades. Hydrogel is a heterogeneous mixture consisting of mainly cross-linked polymers filled with water. It has a wide range of applications in numerous fields, including drug delivery, food additives, contact lens production, wound healing, artificial snow, hygiene products, cell growth and soil conditioners.[287] The various potential applications of the hydrogel are displayed in the Fig. 17. Because of the limited ability of NC to entangle, it is not suitable to be used as a single component hydrogel. However, it can form a gel-like aggregate at high concentration.[288] In addition, the destabilization of NC suspension by adding salts or acids and formation of crosslinks between its chains can lead to the formation of NC hydrogel.[289] Xu *et al.*[290] prepared hydrogel scaffolds for wound healing and tissue regeneration applications by 3D printing. The hydrogel was formed through double crosslinking, the first being *in situ* $CaCl_2$ crosslinking and the second being post-printing using 1,4-butanediol diglycidyl ether. The hydrogel

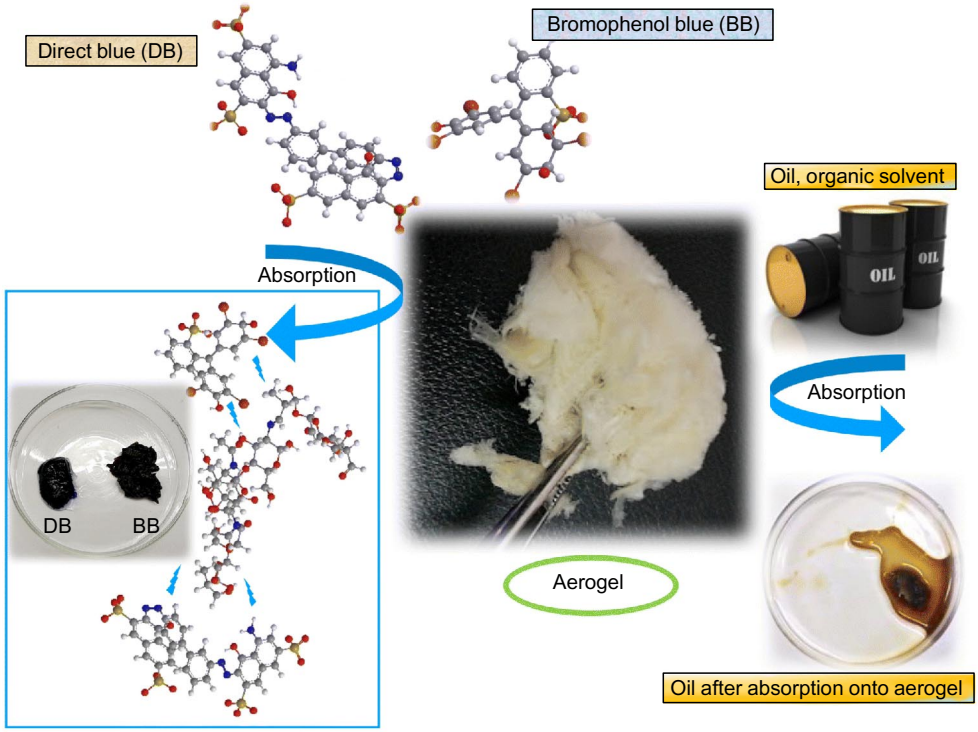

Figure 16. Aerogel based on dialdehyde, CNC/nanobentonite and carboxymethyl chitosan used to remove dye, oil and organic solvents.[286] Published with permission from Springer Nature.

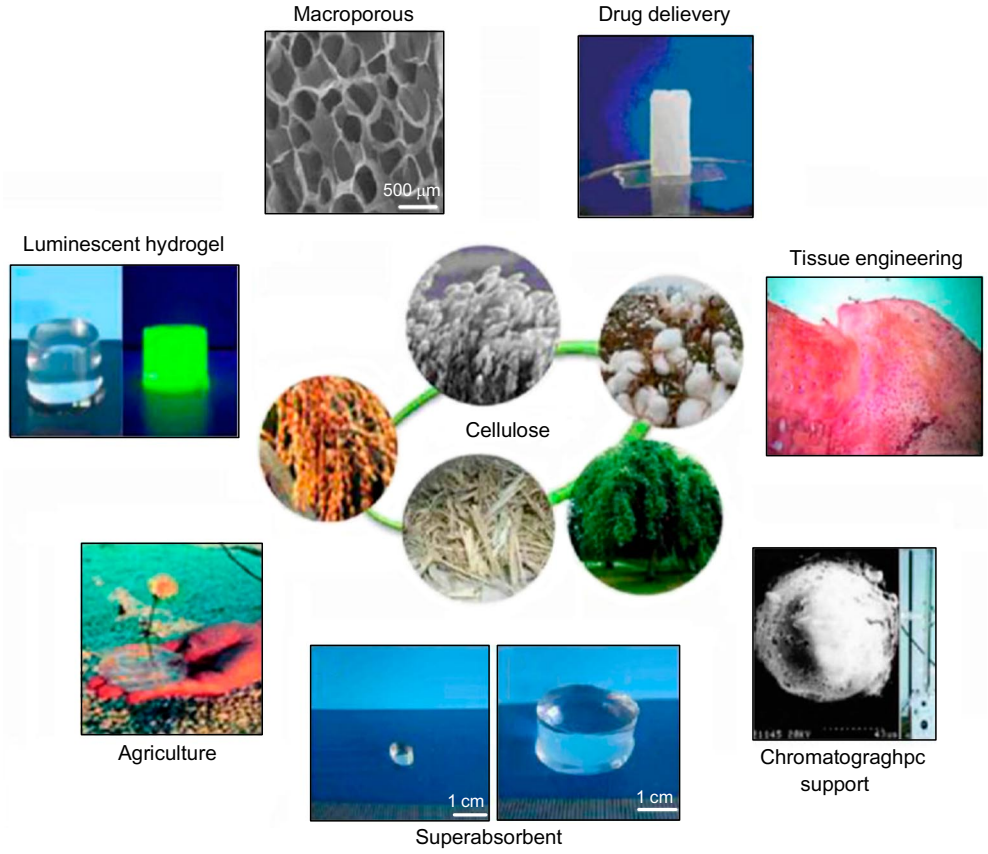

Figure 17. Various applications of hydrogel.[299] Published in accordance with the Creative Commons Attribution license CC BY 4.0.

scaffolds were printed successfully from 1% CNF hydrogel with tunable mechanical strength in the range of 3–8 kPa. Barajas-Ledesma *et al.*[291] prepared carboxylated NC using TEMPO-mediated oxidation. The oxidized fibers were suspended in solutions of different cations (NH_4^+, K^+, Na^+, Mg^{2+}, Zn^{2+}, and Ca^{2+}) to achieve ionic cross-linking and consequently, NC-based hydrogel. The ammonium cation showed the slowest kinetic and the maximum adsorption capacity. The cross-linked carboxylated chitosan and carboxylated NC blend hydrogel beads were prepared through cross-linking of their mixture in a solution of $CaCl_2$. This hydrogel exhibited excellent adsorption capacity for Pb(II) ions reaching 334.92 mg g^{-1} (Ref. 292) Buali *et al.*[293] prepared a hydrogel based on carboxymethyl cellulose filled with NC or nanoclays (namely, montmorillonite and vermiculite) for soil conditioning and nutrient carrier applications. The product was cross-linked using citric acid. The results showed that the lower interaction between the filler and CMC, the greater the crosslinking, and consequently, the higher the water absorption. The hydrogels that contain montmorillonite showed the lowest interaction with carboxymethyl cellulose and the highest reduction in fertilizer loss and the highest water absorption. Thermoreversible gels that can be used for encapsulation and culture of T-cells were prepared from CNC functionalized with a copolymer of *N*,*N*′-dimethylaminoethylmethacrylate and *N*-isopropylacrylamide. The gel was formed at 37 °C and dissociated upon cooling where the cells are allowed to release from the gel, allowing further cell characterization.[294] The drug delivery hydrogel based on NC was produced from CNF and poly(*N*-isopropylacrylamide). The TEMPO-mediate oxidation was used to adjust the carboxyl charge level for pH-responsive hydrogel. The drug release was carried out using methylene blue drug model at temperatures from 20 to 60 °C and a pH range from 2 to 10. The results showed the prepared hydrogel can release the drug on demand.[295] Another drug delivery material was prepared by incorporating gelatine-coated magnetic nanoparticles in gelatine/BC matrix followed by chemical cross-linking using glutaraldehyde. The maximum swelling ratio (1085 ± 12%) was recorded at pH 1.2 in phosphate buffer saline at 37 °C. In addition, under the same conditions, the maximum drug release was 80.77 ± 0.33%.[296] Hydrogel based on amino- and carboxyl-functionalized CNC were prepared. The amino-functionalized CNC formed the hydrogel in an basic environment while the carboxyl-functionalized CNC formed the hydrogel in an acidic environment, where the surface of CNC becomes neutral and the attractive forces based on hydrogen bonding predominate.[297] A PVA-based hydrogel with various concentrations of nanowhisker (CNW) (1, 3, 5 and 7 wt.%), was prepared using Freeze-Thaw technique. This study showed that the addition of CNW to the hydrogel allows to control the pore morphology of the samples without affecting their transparency. The mechanical and thermal properties were improved by adding CNW; the prepared hydrogel can be used as wound dressing.[298]

8. Conclusion

The urgent need for sustainability and environmental protection is driving an ever-increasing interest in the development of biodegradable and renewable materials. Due to its various advantages, NC is frequently used to create high-performance, eco-friendly materials for a variety of applications. This review highlights the value of NC as a precious

natural resource and several significant factors related to its production. The processing parameters involved in pretreatment method for the isolation of cellulose from different lignosellulosic sources, followed by the extraction of NC, are discussed. The advantages and drawbacks of each pretreatment and extraction technique are clarified. The fabrication and characterization techniques of NC-based composites are also considered. The impact of NC on different applications, including sensors, electronics, construction, paper, biomedical, fuel cells, water purification, food packaging, hydrogel, and aerogel applications is presented. The most important obstacle to the use of NC on a larger scale and for wider applications is the high production cost. So, future studies are expected to focus on reducing its high production cost and using non-polluting extraction methods. The cellulose sources such as algae that have highly crystalline cellulose content with low growing cost and higher growing rate may gain more interest. The development of facile and single-step extraction processes involving mild, green, and low-energy-consuming reaction conditions will be a promising goal in the future. Alternative methods for acid hydrolysis are needed to be environmentally friendly to avoid the structural damage and hazardous by-products. Researchers will concentrate on developing green and cost-effective treatment methods, such as those using DES and APS instead of ionic liquids and TEMPO. In addition, techniques such as 3D printing, electrospinning, and Pickering emulsion that can control and adapt the shape and properties of the final composite will get more attention in order to broaden the range of NC polymer composite applications. We anticipate this study to inspire research projects aimed at improving the NC production method and attributes, thereby expanding their industrial applicability and supporting the sustainable use of renewable resources.

Ahmed Abdel-Hakim: idea for the article, literature survey, writing and revision of the manuscript. Reda M. Mourad: idea for the article, writing and revision of the manuscript.

The authors declare no conflict of interests.

9. List of acronyms

AFM — atomic force microscopy,
APS — ammonium persulfate,
BC — bacterial cellulose,
BNC — bacterial nanocellulose,
CMC — cellulose microcrystals,
CMF — cellulose microfibers,
CNC — cellulose nanocrystals,
CNF — cellulose nanofibers,
CrI — crystallinity index,
DES — deep eutectic solvent,
DMA — dynamic mechanical analysis,
DSC — deferential scanning calorimetry,
FTIR — fourier transform infrared spectroscopy,
GO — graphene oxide,
HBA — hydrogen bond acceptor,
HBD — hydrogen bond donor,
IL — ionic liquid,
MC — microcellulose,
MCC — microcrystalline cellulose,
MFC — microfibrillated cellulose,
NC — nanocellulose,
PBAT — poly(butylene adipate-co-terephthalate),
PBS — poly(butylene succinate),
PES — polyethersulfone,
PHA — polyhydroxyalkanoate,
PHB — polyhydroxybutyrate,
PLA — polylactic acid,
PVA — polyvinyl alcohol,
SEM — scanning electron microscopy,
TEM — transmission electron microscopy,
TEMPO — 2,2,6,6-tetramethylpiperidine-1-oxyl radical,
TGA — thermogravimetric analysis,
XRD — X-ray diffraction.

10. References

1. K.G.Moodley, V.Arumugam, A.Barhoum. In *Handbook of Nanocelluloses Classification, Properties, Fabrication, and Emerging Applications*. (Ed. A.Barhoum) *Nanocellulose-Based Materials for Wastewater Treatment*. (Cham: Springer, 2021); https://doi.org/10.1007/978-3-030-62976-2_48-1
2. V.Srivastava, S.Singh, D.Das. *Biodegradable Fibre-Based Composites as Alternative Materials for Sustainable Packaging Design*. (Singapore: Springer, 2022)
3. R.Gheribi, M.A.Gharbi, M.El Ouni, K.Khwaldia. *Food Packag. Shelf Life*, **22**, 100386 (2019)
4. P.Rai, S.Mehrotra, S.Priya, E.Gnansounou, S.K.Sharma. *Bioresource Technol.*, **325**, 124739 (2021)
5. R.Scaffaro, A.Maio, F.Sutera, E.F.Gulino, M.Morreale. *Polymers*, **11**, 651 (2019)
6. M.Zhang, F.Sharaf, L.Chengtao. *Polym. Bull.*, 1 (2022)
7. H.Jia, M.Zhang, Y.Weng, Y.Zhao, C.Li, A.Kanwal. *J. Environment. Sci.*, **103**, 50 (2021)
8. F.Ruggero, R.Gori, C.Lubello. *Waste Manag. Res.*, **37**, 959 (2019)
9. C.Sun, S.Wei, H.Tan, Y.Huang, Y.Zhang. *Chem. Eng. J.*, 136881 (2022)
10. L.Ranakoti, B.Gangil, S.K.Mishra, T.Singh, S.Sharma, R.Ilyas, S.El-Khatib. *Materials*, **15**, 4312 (2022)
11. B.Y.Karlinskii, V.P.Ananikov. *Chem. Soc. Rev.*, **52**, 836 (2023)
12. G.Fernandez-Bunster, P.Pavez. *Molecules*, **27**, 8351 (2022)
13. I.Velzeboer, C.Kwadijk, A.Koelmans. *Environment. Sci. Technol.*, **48**, 4869 (2014)
14. L.Brinchi, F.Cotana, E.Fortunati, J.Kenny. *Carbohydr. Polym.*, **94**, 154 (2013)
15. A.Salam, L.A.Lucia, H.Jameel. *ACS Sustain. Chem. Eng.*, **1**, 1584 (2013)
16. M.Alavi. *e-Polymers*, **19**, 103 (2019)
17. K.-Y.Lee, T.Tammelin, K.Schulfter, H.Kiiskinen, J.Samela, A.Bismarck. *ACS Appl. Mater. Interfaces*, **4**, 4078 (2012)
18. J.George, S.Sabapathi. *Nanotechnol., Sci. Applications*, **8**, 45 (2015)
19. D.Klemm, F.Kramer, S.Moritz, T.Lindström, M.Ankerfors, D.Gray, A.Dorris. *Angew. Chem. Int. Ed.*, **50**, 5438 (2011)
20. M.Alavi, M.Hamidi. *Drug Metabolism Personalized Therapy*, **34** (2019)
21. Â.B.Kraemer, G.M.Parfitt, D.da Silva Acosta, G.E.Bruch, M.F.Cordeiro, L.F.Marins, J.Ventura-Lima, J.M.Monserrat, D.M.Barros. *Toxicol Appl. Pharm.*, **338**, 197 (2018)
22. M.Rad, M.Taran, M.Alavi. *Nano Biomed. Eng.*, **10**, 25 (2018)
23. A.Ferrer, L.Pal, M.Hubbe. *Ind. Crops Prod.*, **95**, 574 (2017)
24. M.N.Norizan, S.S.Shazleen, A.H.Alias, F.A.Sabaruddin, M.R.M.Asyraf, E.S.Zainudin, N.Abdullah, M.S.Samsudin, S.H.Kamarudin, M.N.F.Norrrahim. *Nanomaterials*, **12**, 3483 (2022)
25. S.Padhi, A.Singh, W.Routray. *Rev. Environment. Sci. Bio/Technol.*, 1 (2023)
26. K.Dhali, M.Ghasemlou, F.Daver, P.Cass, B.Adhikari. *Sci. Total Environment*, **775**, 145871 (2021)
27. A.A.B.Omran, A.A.Mohammed, S.Sapuan, R.Ilyas, M.Asyraf, S.S.Rahimian Koloor, M.Petrů. *Polymers*, **13**, 231 (2021)

28. R.Shen, S.Xue, Y.Xu, Q.Liu, Z. Feng, H.Ren, H.Zhai, F.Kong. *Polymers*, **12**, 2113 (2020)
29. T.G.Volova, S.V.Prudnikova, E.G. Kiselev, I.V.Nemtsev, A.D.Vasiliev, A.P.Kuzmin, E.I.Shishatskaya. *Nanomaterials*, **12**, 192 (2022)
30. H.Zhao, L.Zhao, X.Lin, L.Shen. *Carbohydr. Polym.*, **278**, 118968 (2022)
31. H.A.Khalil, A.Bhat, A.I.Yusra. *Carbohydr. Polym.*, **87**, 963 (2012)
32. R.J.Moon, A.Martini, J.Nairn, J.Simonsen, J.Youngblood. *Chem. Soc. Rev.*, **40**, 3941 (2011)
33. A.A.B.Omran, A.A.Mohammed, S.Sapuan, R.Ilyas, M.Asyraf, S.S.Rahimian Koloor, M.Petrů. *Polymers* **13**, 231 (2021)
34. K.Gouda, S.Bhowmik, B.Das. *Rev. Adv. Mater. Sci.*, **60**, 237 (2021)
35. A.B.Perumal, R.B.Nambiar, J.Moses, C.Anandharamakrishnan. *Food Hydrocol., 107484 (2022)*
36. D.Haldar, K.Gayen, D.Sen. *Proc. Biochem.*, **72**, 130 (2018)
37. Z.Ling, W.Tang, Y.Su, C.Huang, C.Lai, A.Kirui, T.Wang, A.D.French, Q.Yong. *Ind. Crops Prod.*, **177**, 114450 (2022)
38. C.J.Chirayil, L.Mathew, S.Thomas. *Rev. Adv. Mater. Sci.*, **37** (2014)
39. D.Haldar, M.K.Purkait. *Carbohydr. Polym.,* **250**, 116937 (2020)
40. S.Tanpichai, F.Phoothong, A.Boonmahitthisud. *Sci. Rep.*, **12**, 1 (2022)
41. S.Tanpichai, S.Mekcham, C.Kongwittaya, W.Kiwijaroun, K.Thongdonsun, C.Thongdeelerd, A.Boonmahitthisud. *J. Nat. Fibers*, 1 (2021)
42. Y.Luo, Y.Li, L.Cao, J.Zhu, B.Deng, Y.Hou, C.Liang, C.Huang, C.Qin, S.Yao. *Biores. Technol.*, **341**, 125757 (2021)
43. J. Ponce, J.G.da Silva Andrade, L.N.dos Santos, M.K.Bulla, B.C.B.Barros, S.L.Favaro, N. Hioka, W.Caetano, V.R.Batistela. *Carbohydr. Polym. Technol. Appl.*, **2**, 100061 (2021)
44. R.Ilyas, S.Sapuan, M.Ishak. *Carbohydr. Polym.*, **181**, 1038 (2018)
45. M.Beroual, D.Trache, O.Mehelli, L.Boumaza, A.F.Tarchoun, M.Derradji, K.Khimeche. *Waste and Biomass Valor.*, **12**, 2779 (2021)
46. A.R.Martin, M.A.Martins, O.R.da Silva, L.H.Mattoso. *Thermochim. Acta*, **506**, 14 (2010)
47. D.García-García, R.Balart, J.Lopez-Martinez, M.Ek, R.Moriana. *Cellulose*, **25**, 2925 (2018)
48. Y.Sun, J.Cheng. *Biores. Technol.*, **83**, 1 (2002)
49. G.Garrote, H.Dominguez, J.Parajo. *Holz als Roh- und Werkstoff*, **57**, 191 (1999)
50. C.Cuissinat, P.Navard. *Cellulose*, **15**, 67 (2008)
51. S.Tanpichai, S.K.Biswas, S.Witayakran, H.Yano. *ACS Sustain. Chem. Eng.*, **7**, 18884 (2019)
52. H.M.Kim, S.G.Wi, S.Jung, Y.Song, H.-J.Bae. *Biores. Technol.*, **175**, 128 (2015)
53. A.F.Tarchoun, D.Trache, T.M.Klapötke. *Int. J. Biolog. Macromol.*, **138**, 837 (2019)
54. Y.W.Chen, H.V.Lee, J.C.Juan, S.-M.Phang. *Carbohydr. Polym.*, **151**, 1210 (2016)
55. A.Mihranyan. *J. Appl. Polym. Sci.*, **119**, 2449 (2011)
56. R.Ek, C.Gustafsson, A.Nutt, T.Iversen, C.Nyström. *J. Mol. Recogn.*, **11**, 263 (1998)
57. A.J.Brown. *J. Chem. Soc., Transactions*, **49**, 432 (1886)
58. Y.Huang, C.Zhu, J.Yang, Y.Nie, C.Chen, D.Sun. *Cellulose*, **21**, 1 (2014)
59. C.Zhong. *Frontiers Bioeng. Biotechnol.*, **8**, 605374 (2020)
60. J.Wang, J.Tavakoli, Y.Tang. *Carbohydr. Polym.*, **219**, 63 (2019)
61. Y.Huang, C.Zhu, J.Yang, Y.Nie, C.Chen, D.Sun. *Cellulose*, **21**, 1 (2014)
62. M.Szymańska-Chargot, M.Chylińska, J.Cybulska, A.Kozioł, P.M.Pieczywek, A.Zdunek. *Carbohydr. Polym.*, **174**, 970 (2017)
63. Y.Yamada, P.Yukphan, H.T.L.Vu, Y.Muramatsu, D.Ochaikul, S.Tanasupawat, Y.Nakagawa. *J. Gen. Appl. Microbiol.*, **58**, 397 (2012)
64. D.Lin, Z.Liu, R.Shen, S.Chen, X.Yang. *Int. J. Biol. Macromol.*, **158**, 1007 (2020)
65. F.Mohammadkazemi, M.Azin, A.Ashori. *Carbohydr. Polym.*, **117**, 518 (2015)
66. H.M.Azeredo, H.Barud, C.S.Farinas, V.M.Vasconcellos, A.M.Claro. *Frontiers Sustain. Food Syst.*, **3**, 7 (2019)
67. I.Cielecka, M.Szustak, H.Kalinowska, E.Gendaszewska-Darmach, M.Ryngajłło, W.Maniukiewicz, S.Bielecki. *Cellulose*, **26**, 5409 (2019)
68. I.Reiniati, A.N. Hrymak, A.Margaritis. *Critical Rev. Biotechnol.*, **37**, 510 (2017)
69. P.Cazón, M.Vázquez. *Food Hydrocolloids*, **113**, 106530 (2021)
70. Y.Hu, J.M.Catchmark, E.A.Vogler. *Biomacromolecules*, **14**, 3444 (2013)
71. Y.E.Öz, M.Kalender. *Int. J. Biol. Macromol.*, **225**, 1306 (2023)
72. N.Berrill. *J. Morphology*, **81**, 269 (1947)
73. Y.Zhao, J.Li. *Cellulose*, **21**, 3427 (2014)
74. Y.Nishiyama, P.Langan, H.Chanzy. *J. Am. Chem. Soc.*, **124**, 9074 (2002)
75. P.Phanthong, P.Reubroycharoen, X.Hao, G.Xu, A.Abudula, G.Guan. *Carbon Res. Conversion*, **1**, 32 (2018)
76. A.F.Jozala, L.C.de Lencastre-Novaes, A.M.Lopes, V.de Carvalho Santos-Ebinuma, P.G.Mazzola, A.Pessoa Jr., D.Grotto, M.Gerenutti, M.V.Chaud. *Appl. Microbiol. Biotech.*, **100**, 2063 (2016)
77. E.Abu-Danso, V.Srivastava, M.Sillanpää, A.Bhatnagar. *Int. J. Biol. Macromol.*, **102**, 248 (2017)
78. S.Singh, K.K.Gaikwad, S.-I.Park, Y.S.Lee. *Int. J. Biol. Macromol.*, **99**, 506 (2017)
79. F.K.Liew, S.Hamdan, M.Rahman, M.Rusop, J.C.H.Lai, M.Hossen. *J. Chem.*, **2015** (2015)
80. N.Y.Abu-Thabit, A.A.Judeh, A.S.Hakeem, A.Ul-Hamid, Y.Umar, A.Ahmad. *Int. J. Biol. Macromol.*, **155**, 730 (2020)
81. A.Bismarck, A.K.Mohanty, I.Aranberri-Askargorta, S.Czapla, M.Misra, G.Hinrichsen, J.Springer. *Green Chem.*, **3**, 100 (2001)
82. C.Dash, A.Das, D.Kumar Bisoyi. *J. Composite Mater.*, **54**, 3313 (2020)
83. M.M.Rahman, A.K.Mallik, M.A.Khan. *J. Appl. Polym. Sci.*, **105**, 3077 (2007)
84. J. Sun, X.Sun, H.Zhao, R.Sun. *Polym. Degrad. Stabil.*, **84**, 331 (2004)
85. C.Trilokesh, K.B.Uppuluri. *Sci. Rep.*, **9**, 1 (2019)
86. M.Bassyouni. *J. Reinforced Plastics Compos.*, **37**, 1402 (2018)
87. Y.W.Chen, H.V.Lee, S.B.Abd Hamid. *Carbohydr. Polym.*, **157**, 1511 (2017)
88. F.Jiang, Y.-L.Hsieh. *Carbohydr. Polym.*, **122**, 60 (2015)
89. J.S.Kim, Y.Lee, T.H.Kim. *Biores. Technol.*, **199**, 42 (2016)
90. H.-M.Ng, L.T.Sin, T.-T.Tee, S.-T.Bee, D.Hui, C.-Y.Low, A.Rahmat. *Composites Part B: Eng.*, **75**, 176 (2015)
91. D.P.Maurya, A.Singla, S.Negi. *3 Biotech*, **5**, 597 (2015)
92. A.Bhatnagar, M.Sain. *J. Reinforced Plastics Compos.*, **24**, 1259 (2005)
93. J.Baruah, B.K.Nath, R.Sharma, S.Kumar, R.C.Deka, D.C.Baruah, E.Kalita. *Frontiers in Energy Res.*, **6**, 141 (2018)
94. S.Karimi, P.M.Tahir, A.Karimi, A.Dufresne, A.Abdulkhani. *Carbohydr. Polym.*, **101**, 878 (2014)
95. S.Nandi, P.Guha. *J. Packaging Technol. Res.*, **2**, 149 (2018)
96. Z.Karim, S.Afrin, Q.Husain, R.Danish. *Crit. Rev. Biotechnol.*, **37**, 355 (2017)
97. S.K.Tripathi, N.K.Bhardwaj, H.Roy Ghatak. *Ozone: Sci. Eng.*, **41**, 137 (2019)
98. D.Kaur, N.K.Bhardwaj, R.K.Lohchab. *J. Clean. Produc.*, **170**, 174 (2018)

99. H.R.Lee, R.J.Kazlauskas, T.H.Park. *Sci. Rep.*, **7**, 1 (2017)
100. M.Rosa, E.Medeiros, J. Malmonge, K.Gregorski, D.Wood, L.Mattoso, G.Glenn, W.Orts, S.Imam. *Carbohydr. Polym.*, **81**, 83 (2010)
101. A.De Campos, A.C.Correa, D.Cannella, E.de M Teixeira, J.M.Marconcini, A.Dufresne, L.H.Mattoso, P.Cassland, A.R.Sanadi. *Cellulose*, **20**, 1491 (2013)
102. M.Jonoobi, J.Harun, M.Mishra, K.Oksman. *BioRes.*, **4**, 626 (2009)
103. N.Johar, I.Ahmad, A.Dufresne. *Ind. Crops Prod.*, **37**, 93 (2012)
104. A.Sonia, K.P.Dasan, R.Alex. *Chem. Eng. J.*, **228**, 1214 (2013)
105. B.Bahrami, T.Behzad, A.Zamani, P.Heidarian, B.Nasri-Nasrabadi. *J. Polym. Environment.*, **26**, 4085 (2018)
106. L.Zhong, S.Fu, F.Li, H.Zhan. *BioRes.*, **5**, 2431 (2010)
107. P.Tao, Y.Zhang, Z.Wu, X.Liao, S.Nie. *Carbohydr. Polym.*, **214**, 1 (2019)
108. H.Jørgensen, J.B.Kristensen, C.Felby. *Biofuels, Bioprod. Biorefin.*, **1**, 119 (2007)
109. X.Tong, W.Shen, X.Chen, M.Jia, J.-C.Roux. *J. Appl. Polym. Sci.*, **137**, 48407 (2020)
110. X.-Q.Chen, G.-X.Pang, W.-H.Shen, X.Tong, M.-Y.Jia. *Carbohydr. Polym.*, **207**, 713 (2019)
111. M.A.Yassin, A.A.M.Gad, A.F.Ghanem, M.H.Abdel Rehim. *Carbohydr. Polym.*, **205**, 255 (2019)
112. J. Peyre, T.Pääkkönen, M.Reza, E.Kontturi. *Green Chem.*, **17**, 808 (2015)
113. V.Barbash, O.Yashchenko, A.Gondovska, I.Deykun. *Appl. Nanosci.*, **12** (2021)
114. F.Fan, M.Zhu, K.Fang, E.Cao, Y.Yang, J. Xie, Z.Deng, Y.Chen, X.Cao. *Cellulose*, **29** (2021)
115. M.Shahriari-Khalaji, G.Li, L.Liu, M.Sattar, L.Chen, C.Zhong, F.F.Hong. *Carbohydr. Polym.*, **287**, 119266 (2022)
116. E.Indarti, R.Rohaizu, W.Wanrosli. *Int. J. Biol. Macromol.*, **135**, 106 (2019)
117. H.Wang, M.Pudukudy, Y.Ni, Y.Zhi, H.Zhang, Z.Wang, Q.Jia, S.Shan. *Cellulose*, **27**, 657 (2020)
118. A.Adel, A.El-Shafei, A.Ibrahim, M.Al-Shemy. *Ind. Crops Prod.*, **124**, 155 (2018)
119. M.Marwanto, M.I.Maulana, F.Febrianto, N.J.Wistara, S.Nikmatin, N. Masruchin, L.H.Zaini, S.-H.Lee, N.H.Kim. *Wood Sci. Technol.*, **55**, 1319 (2021)
120. J.N.Putro, F.E.Soetaredjo, S.-Y.Lin, Y.-H.Ju, S.Ismadji. *RSC Adv.*, **6**, 46834 (2016)
121. A.M.da Costa Lopes, K.G.João, D.F.Rubik, E.Bogel-Łukasik, L.C.Duarte, J. Andreaus, R.Bogel-Łukasik. *Biores. Technol.*, **142**, 198 (2013)
122. A.P.Carneiro, O.Rodriguez, E.A.Macedo. *Biores. Technol.*, **227**, 188 (2017)
123. M.Babicka, M.Woźniak, K.Dwiecki, S.Borysiak, I.Ratajczak. *Molecules*, **25**, 1544 (2020)
124. D.M.Correia, L.C.Fernandes, M.M.Fernandes, B.Hermenegildo, R.M.Meira, C.Ribeiro, S.Ribeiro, J.Reguera, S.Lanceros-Méndez. *Nanomaterials*, **11**, 2401 (2021)
125. I.V.Pletnev, S.V.Smirnova, A.V.Sharov, Y.A.Zolotov. *Russ. Chem. Rev.*, **90**, 1109 (2021)
126. Y.Dai, J.van Spronsen, G.-J. Witkamp, R.Verpoorte, Y.H.Choi. *Anal. Chim. Acta*, **766**, 61 (2013)
127. H.Zhang, J.Lang, P.Lan, H.Yang, J.Lu, Z.Wang. *Materials*, **13**, 278 (2020)
128. Q.Liu, T.Yuan, Q.-j.Fu, Y.-y.Bai, F.Peng, C.-l.Yao. *Cellulose*, **26**, 9447 (2019)
129. J.A.Sirviö, M.Visanko, H.Liimatainen. *Green Chem.*, **17**, 3401 (2015)
130. S.Tanpichai, S.Witayakran, A.Boonmahitthisud. *J. Environment. Chem. Eng.*, **7**, 102836 (2019)
131. F.Yeganeh, N.Chiewchan, W.Chonkaew. *Cellulose*, **29**, 2333 (2022)
132. A.Suzuki, C.Sasaki, C.Asada, Y.Nakamura. *BioRes.*, **12**, 7628 (2017)
133. I.Hongrattanavichit, D.Aht-Ong. *J. Cleaner Production*, **277**, 123471 (2020)
134. B.L.Peng, N.Dhar, H.Liu, K.Tam. *Canadian J. Chem. Eng.*, **89**, 1191 (2011)
135. N.Lavoine, I.Desloges, A.Dufresne, J.Bras. *Carbohydr. Polym.*, **90**, 735 (2012)
136. D.Bondeson, A.Mathew, K.Oksman. *Cellulose*, **13**, 171 (2006)
137. P.Lu, Y.-L.Hsieh. *Carbohydr. Polym.*, **82**, 329 (2010)
138. S.Maiti, J. Jayaramudu, K.Das, S.M.Reddy, R.Sadiku, S.S.Ray, D.Liu. *Carbohydr. Polym.*, **98**, 562 (2013)
139. A.F.Tarchoun, D.Trache, T.M.Klapötke, M.Derradji, W.Bessa. *Cellulose*, **26**, 7635 (2019)
140. A.Dufresne. *Nat. Polym.*, **2**, 1 (2012)
141. H.A.Khalil, Y.Davoudpour, M.N.Islam, A.Mustapha, K.Sudesh, R.Dungani, M.Jawaid. *Carbohydr. Polym.*, **99**, 649 (2014)
142. J. Li, X.Wei, Q.Wang, J.Chen, G.Chang, L.Kong, J.Su, Y.Liu. *Carbohydr. Polym.*, **90**, 1609 (2012)
143. Y.Wang, X.Wei, J. Li, F.Wang, Q.Wang, Y.Zhang, L.Kong. *Ind. Crops Prod.*, **104**, 237 (2017)
144. Y.Ni, J.Li, L.Fan. *Int. J. Biol. Macromol.*, **149**, 617 (2020)
145. Q.Chen, Y.Liu, G.Chen. *Cellulose*, **26**, 2425 (2019)
146. H.Khalil, Y.Davoudpour, N.S.Aprilia, A.Mustapha, S.Hossain, N.Islam, R.Dungani. *Nanocellulose Polym. Nanocomp.*, 273 (2014)
147. E.Syafri, E.Yulianti, M.Asrofi, H.Abral, S.Sapuan, R.Ilyas, A.Fudholi. *J. Mater. Res. Technol.*, **8**, 6223 (2019)
148. R.Zhu, V.Yadama. *J. Polym. Environment*, **26**, 1012 (2018)
149. H.J. Kim, S.Lee, J.Kim, R.J.Mitchell, J.H.Lee. *Biores. Technol.*, **144**, 50 (2013)
150. M.Ago, T.Endo, T.Hirotsu. *Cellulose*, **11**, 163 (2004)
151. A.V.Rane, K.Kanny, V.Abitha, S.Thomas. In *Synthesis of Inorganic Nanomaterials*. (Eds S.M.Bhagyaraj, O.S.Oluwafemi, N.Kalarikkal, S.Thomas) (Elsevier, 2018). P. 121
152. J.Sapkota, S.Kumar, C.Weder, E.J.Foster. *Macromol. Mater. Eng.*, **300**, 562 (2015)
153. J.Bacalhau, T.Cunha, C.Afonso. *Effect of Ni Content on the Hardenability of a Bainitic Steel for Plastics Processing*. (24th ABCM International Congress of Mechanical Engineering, 2017); https://doi.org/10.26678/ABCM.COBEM2017.COB17-1174
154. K.Oksman, Y.Aitomäki, A.P.Mathew, G.Siqueira, Q.Zhou, S.Butylina, S.Tanpichai, X.Zhou, S.Hooshmand. *Composites Part A: Appl. Sci. Manufacturing*, **83**, 2 (2016)
155. Y.Aitomäki, K.Oksman. *Reac. Functional Polym.*, **85**, 151 (2014)
156. Noorfarisya Izma Jeffri, Nurul Fazita M. R., Cheu Peng Leh, Rokiah Hashim, Mohamad Haafiz M.K, Mazlan Ibrahim, Guan Seng Tay, Takamitsu Arai, Kumar Sudesh, Akihiko Kosugi. *Polym. Compos.*, **24**, 8 (2023)
157. T.Ambone, A.Torris, K.Shanmuganathan. *Polym. Eng. Sci.*, **60**, 1842 (2020)
158. R.Palucci Rosa, G.Rosace, R.Arrigo, G.Malucelli. *Polymers*, **14**, 1886 (2022)
159. Y.Zhou, F.Wang, Z.Yang, X.Hu, Y.Pan, Y.Lu, M.Jiang. *Ind. Crops Prod.*, **182**, 114831 (2022)
160. H.Wang, L.Kong, G.R.Ziegler. *Food Hydrocolloids*, **90**, 90 (2019)
161. A.Ashori, F.Rafieyan, F.Kian, M.Jonoobi, K.Rezaei Tavabe. *Polym. Compos.*, **40**, E835 (2019)
162. L.Ge, J.Yin, D.Yan, W.Hong, T.Jiao. *ACS Omega*, **6**, 4958 (2021)
163. J.Yan, T.Bai, Y.Yue, W.Cheng, L.Bai, D.Wang, J.Lu, M.Cao, S.Q.Shi, S.Huan. *Compos. Sci. Technol.*, **224**, 109490 (2022)

164. X.Tan, Q.Peng, K.Yang, T.Yang, J.Saskova, J.Wiener, M.Venkataraman, J.Militky, W.Xiong, J.Xu. *Alexandria Eng. J.*, **61**, 4529 (2022)
165. X.Ji, J.Guo, F.Guan, Y.Liu, Q.Yang, X.Zhang, Y.Xu. *Gels*, **7**, 223 (2021)
166. B.Sun, D.Chao, C.Wang. *Chem. Res. Chin. Univ.*, **38**, 1005 (2022)
167. S.K.Biswas, H.Sano, X.Yang, S.Tanpichai, M.I.Shams, H.Yano. *Adv. Opt. Mater.*, **7**, 1900532 (2019)
168. S.K.Biswas, S.Tanpichai, S.Witayakran, X.Yang, M.I.Shams, H.Yano. *ACS Nano*, **13**, 2015 (2019)
169. M.Y.Koroleva, E.V.e.Yurtov. *Russ. Chem. Rev.*, **91**, RCR5024 (2022)
170. M.J.John, N.Dyanti, T.Mokhena, V.Agbakoba, B.Sithole. *Materials*, **14**, 3462 (2021)
171. O.Platnieks, S.Gaidukovs, A.Barkane, A.Sereda, G.Gaidukova, L.Grase, V.K.Thakur, I.Filipova, V.Fridrihsone, M.Skute. *Polymers*, **12**, 1472 (2020)
172. I.Mahendra, B.Wirjosentono, T.Tamrin, H.Ismail, J.Mendez, V.Causin. *J. Thermoplast. Compos. Mater.*, 0892705720959129 (2020)
173. W.Chawalitsakunchai, P.Dittanet, S.Loykulnant, P.Sae-oui, S.Tanpichai, A.Seubsai, P.Prapainainar. *Mater. Today Commun.*, **28**, 102594 (2021)
174. S.Xu, N.Girouard, G.Schueneman, M.L.Shofner, J.C.Meredith. *Polymer*, **54**, 6589 (2013)
175. M.Guimarães Junior, F.G.Teixeira, G.H.D.Tonoli. *Cellulose*, **25**, 1823 (2018)
176. J.Joy, C.Jose, S.B.Varanasi, M.P.Lovely, T.Sabu, S.Pilla. *J. Renew. Mater.*, **4**, 351 (2016)
177. G.Mármol, C.Gauss, R.Fangueiro. *Molecules*, **25**, 4653 (2020)
178. B.Zhang, C.Huang, H.Zhao, J.Wang, C.Yin, L.Zhang, Y.Zhao. *Polymers*, **11**, 2063 (2019)
179. J.Yu, Y.Jin, G.Liu, F.Hua, Y.Lv. *J. Appl. Polym. Sci.*, **139**, 52130 (2022)
180. L.Cui, L.Yi, N.Hegyesi, Y.Wang, X.Sui, B.Pukánszky. *Ind. Crops Prod.*, **187**, 115411 (2022)
181. M.Latif, Y.Jiang, B.Kumar, J.M.Song, H.C.Cho, J.Kim. *Adv. Mater. Interfaces*, 2200280 (2022)
182. D.Mohan, N.F.Khairullah, Y.P.How, M.S.Sajab, H.Kaco. *Polymers*, **12**, 986 (2020)
183. A.Abdel-Hakim, R.M.Mourad. *Polym. Compos.*, **41**, 1435 (2020)
184. A.Abdel-Hakim, E.H.Awad, K.F.El-Nemr, T.M.El-Basheer. *Rad. Phys. Chem.*, **189**, 109768 (2021)
185. Y.Zhou, S.Fu, L.Zheng, H.Zhan. *Express Polym. Lett.*, **6** (2012)
186. E.Abraham, M.S.Thomas, C.John, L.Pothen, O.Shoseyov, S.Thomas. *Ind. Crops Prod.*, **51**, 415 (2013)
187. J.P.Reddy, J.-W.Rhim. *Carbohydr. Polym.*, **110**, 480 (2014)
188. M.J. Smith, N.A.Peppas. *Polymer*, **26**, 569 (1985)
189. R.A.Khan, S.Salmieri, D.Dussault, J.Uribe-Calderon, M.R.Kamal, A.Safrany, M.Lacroix. *J. Agricul. Food Chem.*, **58**, 7878 (2010)
190. S.Varshney, N.Mishra, M.Gupta. *Polym. Compos.*, **42**, 3660 (2021)
191. X.Ju, M.Bowden, E.E.Brown, X.Zhang. *Carbohydr. Polym.*, **123**, 476 (2015)
192. L.Segal, J.J. Creely, A.Martin Jr., C.Conrad. *Textile Res. J.*, **29**, 786 (1959)
193. A.D.French, M.Santiago Cintrón. *Cellulose*, **20**, 583 (2013)
194. A.D.French. *Cellulose*, **27**, 5445 (2020)
195. J.Lngford, A.Wilson. *J. Appl. Cryst.*, **11**, 102 (1978)
196. P.Scherrer. *Ges Wiss Göttingen*, **26**, 98 (1918)
197. R.Khoo, H.Ismail, W.Chow. *Procedia Chem.*, **19**, 788 (2016)
198. N.Saba, F.Mohammad, M.Pervaiz, M.Jawaid, O.Alothman, M.Sain. *Int. J. Biol. Macromol.*, **97**, 190 (2017)
199. R.Kumar, B.Rai, S.Gahlyan, G.Kumar. *Express Polym. Lett.*, **15**, 104 (2021)
200. P.G.Marakana, A.Dey, B.Saini. *J. Environment. Chem. Eng.*, **9**, 106606 (2021)
201. A.Mandal, D.Chakrabarty. *Polym. Compos.*, **38**, 1720 (2017)
202. A.Kardam, K.R.Raj, S.Srivastava, M.Srivastava. *Clean Technol. Environment. Policy*, **16**, 385 (2014)
203. M.Bulota, S.Tanpichai, M.Hughes, S.J.Eichhorn. *ACS Appl. Mater. Interfaces*, **4**, 331 (2012)
204. R.Rusli, K.Shanmuganathan, S.J. Rowan, C.Weder, S.J.Eichhorn. *Biomacromolecules*, **11**, 762 (2010)
205. S.Tanpichai, W.W.Sampson, S.J.Eichhorn. *Compos. Part A: Appl. Sci. Manufacturing*, **43**, 1145 (2012)
206. A.G.de Souza, G.F.de Lima, V.K.Rangari, D.dos Santos Rosa. *Polym. Compos.*, **41**, 4340 (2020)
207. I.Vroman, L.Tighzert. *Materials*, **2**, 307 (2009)
208. G.Wächtershäuser. *Microbiol. Rev.*, **52**, 452 (1988)
209. A.-C.Albertsson, S.Karlsson. *Prog. Polym. Sci.*, **15**, 177 (1990)
210. Z.Karim, S.Afrin. *Cell Develop. Biol.*, **4**, 1 (2015)
211. A.A.Kulkarni, P.S.Rao. *Nanomater. Tissue Eng.: Fabrication Applications*, 27 (2013)
212. C.Balalakshmi, S.Jeyachandran. In *Handbook of Nanocelluloses Classification, Properties, Fabrication, and Emerging Applications*. (Ed. A.Barhoum) *Advances of Nanocellulose in Biomedical Applications*. (Cham: Springer, 2022); https://doi.org/10.1007/978-3-030-62976-2_35-1
213. M.Čolić, S.Tomić, M.Bekić. *Immunol. Lett.*, **222**, 80 (2020)
214. N.Stoudmann, M.Schmutz, C.Hirsch, B.Nowack, C.Som. *Nanotoxicology*, **14**, 1241 (2020)
215. C.Ventura, F.Pinto, A.F.Lourenço, P.J.T.Ferreira, H.Louro, M.J.Silva. *Cellulose*, **27**, 5509 (2020)
216. F.A.Sabaruddin, M.Paridah, S.Sapuan, R.Ilyas, S.H.Lee, K.Abdan, N.Mazlan, A.S.M.Roseley, H.Abdul Khalil. *Polymers*, **13**, 116 (2020)
217. R.Weishaupt, G.Siqueira, M.Schubert, M.M.Kämpf, T.Zimmermann, K.Maniura-Weber, G.Faccio. *Adv. Functional Mater.*, **27**, 1604291 (2017)
218. W.Yin, H.Cui, Z.Yang, C.Li, M.She, B.Yin, J. Li, G.Zhao, Z.Shi. *Sensors and Actuators B: Chem.*, **157**, 675 (2011)
219. P.A.Nizam, D.A.Gopakumar, Y.B.Pottathara, D.Pasquini, A.Nzihou, S.Thomas. In *Nanocellulose Based Composites for Electronics*. (Eds S.Thomas, Y.B.Pottathara). (Elsevier, 2021). P. 15
220. Y.Habibi, L.A.Lucia, O.J. Rojas. *Chem. Rev.*, **110**, 3479 (2010)
221. V.Mohanta, G.Madras, S.Patil. *ACS Appl. Mater. Interfaces*, **6**, 20093 (2014)
222. N.Shahi, E.Lee, B.Min, D.-J.Kim. *Sensors*, **21**, 4415 (2021)
223. A.Kafy, K.K.Sadasivuni, A.Akther, S.-K.Min, J.Kim. *Mater Lett.*, **159**, 20 (2015)
224. K.k. Sadasivuni, A.Kafy, H.C.Kim, H.-U. Ko, S.Mun, J.Kim. *Synthetic Metals*, **206** (2015)
225. J.Han, K.Lu, Y.Yue, C.Mei, C.Huang, Q.Wu, X.Xu. *Ind. Crops Prod.*, **128**, 94 (2019)
226. D.Y.Liu, G.Sui, D.Bhattacharyya. *Compos. Sci. Technol.*, **99**, 31 (2014)
227. W.Zheng, R.Lv, B.Na, H.Liu, T.Jin, D.Yuan. *J. Mater. Chem. A*, **5**, 12969 (2017)
228. S.Zhang, R.Fu, Y.Gu, L.Dong, J.Li, S.Chen. *J. Mater. Sci.: Mater. Electron.*, **28**, 10158 (2017)
229. Y.Zhang, Z.Shang, M.Shen, S.P.Chowdhury, A.Ignaszak, S.Sun, Y.Ni. *ACS Sustain. Chem. Eng.*, **7**, 11175 (2019)
230. W.Yang, L.Jiao, W.Liu, Y.Deng, H.Dai. *Cellulose*, **25**, 5909 (2018)
231. Y.J. Kang, H.Chung, C.-H.Han, W.Kim. *Nanotechnology*, **23**, 065401 (2012)
232. M.Fukuhara, T.Kuroda, F.Hasegawa, T.Hashida, M.Takeda, N.Fujima, M.Morita, T.Nakatani. *Sci. Rep.*, **11**, 6436 (2021)
233. M.L.Hassan, A.F.Ali, A.H.Salama, A.M.Abdel-Karim. *J. Phys. Org. Chem.*, **32**, e3897 (2019)
234. T.Jie. *Cellulose*, **26**, 6087 (2019)

235. S.Ji, J.Jang, E.Cho, S.-H.Kim, E.-S.Kang, J.Kim, H.-K.Kim, H.Kong, S.-K.Kim, J.-Y.Kim, J.-U.Park. *Adv. Mater.*, **29**, 1700538 (2017)
236. Y.B.Pottathara, V.Bobnar, M.Finšgar, Y.Grohens, S.Thomas, V.Kokol. *Polymer*, **147**, 260 (2018)
237. Y.B.Pottathara, S.Thomas, N.Kalarikkal, T.Griesser, Y.Grohens, V.Bobnar, M.Finšgar, V.Kokol, R.Kargl. *New J. Chem.*, **43**, 681 (2019)
238. H.T.Nguyen, A.S.Sidorkin, S.D.Milovidova, O.V.Rogazinskaya. *Ferroelectrics*, **501**, 180 (2016)
239. V.P.Anju, S.K.Narayanankutty. *AIP Adv.*, **6**, 015109 (2016)
240. X.Zeng, L.Deng, Y.Yao, R.Sun, J. Xu, C.-P.Wong. *J. Mater. Chem. C*, **4**, 6037 (2016)
241. J.Tao, S.A.Cao. *RSC Adv.*, **10**, 10799 (2020)
242. O.A.T.Dias, S.Konar, A.L.Leão, W.Yang, J.Tjong, M.Sain. *Frontiers Chem.*, **8**, 420 (2020)
243. Z.Cai, R.Li, X.Xu, G.Sun, X.Zhuang, Y.Liu, B.Cheng. *Polymer*, **156**, 179 (2018)
244. X.Xu, R.Li, C.Tang, H.Wang, X.Zhuang, Y.Liu, W.Kang, L.Shi. *Carbohydr. Polym.*, **184**, 299 (2018)
245. T.Bayer, B.V.Cunning, R.Selyanchyn, M.Nishihara, S.Fujikawa, K.Sasaki, S.M.Lyth. *Chem. Mater.*, **28**, 4805 (2016)
246. A.Sriruangrungkamol, W.Chonkaew. *Polym. Bull.*, **78**, 3705 (2021)
247. A.Priyangga, A.B.Pambudi, L.Atmaja, J.Jaafar. *Mater. Today: Proceedings*, **46**, 1998 (2021)
248. C.Vilela, J.D.Morais, A.C.Q.Silva, D.Muñoz-Gil, F.M.Figueiredo, A.J.Silvestre, C.S.Freire. *Nanomaterials*, **10**, 1713 (2020)
249. A.Priyangga, L.Atmaja, M.Santoso, J.Jaafar, H.Ilbeygi. *RSC Adv.*, **12**, 14411 (2022)
250. A.Dufresne. *Curr. Forestry Rep.*, **5**, 76 (2019)
251. M.E.Bakkari, V.Bindiganavile, J.Goncalves, Y.Boluk. *Carbohydr. Polym.*, **203**, 238 (2019)
252. P.Wang, N.Aliheidari, X.Zhang, A.Ameli. *Carbohydr. Polym.*, **218**, 103 (2019)
253. A.L.Missio, C.G.Otoni, B.Zhao, M.Beaumont, A.Khakalo, T.Kämäräinen, S.H.Silva, B.D.Mattos, O.J.Rojas. *ACS Sustainable Chem. Eng.*, **10**, 10303 (2022)
254. X.Ma, S.Tian, X.Li, H.Fan, S.Fu. *Cellulose*, **28**, 8027 (2021)
255. F.Ren, H.Guo, Z.-Z.Guo, Y.-L.Jin, H.-J.Duan, P.-G.Ren, D.-X.Yan. *Polymers*, **11**, 1486 (2019)
256. V.Barbash, O.Yashchenko. *Appl. Nanosci.*, **10**, 2705 (2020)
257. W.Perdoch, Z.Cao, P.Florczak, R.Markiewicz, M.Jarek, K.Olejnik, B.Mazela. *Molecules*, **27**, 4696 (2022)
258. M.F.F.Pego, M.L.Bianchi, P.K.Yasumura. *Wood Sci. Technol.*, **54**, 1587 (2020)
259. J.Tang, L.Bao, X.Li, L.Chen, F.F.Hong. *J. Mater. Chem. B*, **3**, 8537 (2015)
260. H.Vakilian, E.A.Rojas, L.H.Rezaei, M.Behmanesh. *Rep. Biochem. Mol. Biol.*, **9**, 297 (2020)
261. J.P.Carvalho, A.C.Silva, V.Bastos, H.Oliveira, R.J. Pinto, A.J.Silvestre, C.Vilela, C.S.Freire. *Nanomaterials*, **10**, 628 (2020)
262. R.Ghafari, M.Jonoobi, L.M.Amirabad, K.Oksman, A.R.Taheri. *Int. J. Biol. Macromol.*, **136**, 796 (2019)
263. G.Sarkar, J.T.Orasugh, N.R.Saha, I.Roy, A.Bhattacharyya, A.K.Chattopadhyay, D.Rana, D.Chattopadhyay. *New J. Chem.*, **41**, 15312 (2017)
264. R.Reshmy, E.Philip, S.A.Paul, A.Madhavan, R.Sindhu, P.Binod, A.Pandey, R.Sirohi. *Rev. Environment. Sci. Bio/Technol.*, **19**, 779 (2020)
265. A.Agarwal, B.Shaida, M.Rastogi, N.B.Singh. *Chem. Africa*, 1 (2022)
266. X.He, W.Lu, C.Sun, H.Khalesi, A.Mata, R.Andaleeb, Y.Fang. *Carbohydr. Polym.*, **255**, 117334 (2021)
267. F.A.G.Soares da Silva, M.Matos, F.Dourado, M.A.M.Reis, P.C.Branco, F.Poças, M.Gama. *J. Sci. Food Agriculture*, **102** (3), 1077 (2023)
268. D.Maresca, G.Mauriello. *Foods*, **11**, 3051 (2022)
269. G.Lavrič, A.Oberlintner, I.Filipova, U.Novak, B.Likozar, U.Vrabič-Brodnjak. *Polymers*, **13**, 2523 (2021)
270. F.Lu, H.Yu, C.Yan, J.Yao. *RSC Adv.*, **6**, 46008 (2016)
271. L.R.Mugwagwa, A.F.Chimphango. *Food Packag. Shelf Life*, **31**, 100795 (2022)
272. J.Heidarbeigi, H.Afshari, A.Borghei. *J. Thermoplast. Compos. Mater.*, **34**, 396 (2021)
273. F.Rafieian, M.Jonoobi, Q.Yu. *Cellulose*, **26**, 3359 (2019)
274. H.Gholami Derami, Q.Jiang, D.Ghim, S.Cao, Y.J.Chandar, J.J.Morrissey, Y.-S.Jun, S.Singamaneni. *ACS Appl. Nano Mater.*, **2**, 1092 (2019)
275. S.Huang, M.-B.Wu, C.-Y.Zhu, M.-Q.Ma, J.Yang, J.Wu, Z.-K.Xu. *ACS Sustain. Chem. Eng.*, **7**, 12315 (2019)
276. W.Zhu, M.Han, D.Kim, Y.Zhang, G.Kwon, J.You, C.Jia, J.Kim. *Environment. Res.*, **205**, 112417 (2022)
277. T.Shahnaz, D.Bedadeep, S.Narayanasamy. *Int. J. Biol. Macromol.*, **200**, 162 (2022)
278. C.Chen, C.Li, D.Yu, M.Wu. *Cellulose*, **29**, 245 (2022)
279. M.Zhang, M.Li, Q.Xu, W.Jiang, M.Hou, L.Guo, N.Wang, Y.Zhao, L.Liu. *Ind. Crops Prod.*, **179**, 114701 (2022)
280. Z.Zhu, S.Fu, N.Lavoine, L.A.Lucia. *Carbohydr. Polym.*, **247**, 116722 (2020)
281. G.Zhu, L.Giraldo Isaza, B.Huang, A.Dufresne. *ACS Sustain. Chem. Eng.*, **10**, 2397 (2022)
282. F.Rafieian, M.Hosseini, M.Jonoobi, Q.Yu. *Cellulose*, **25**, 4695 (2018)
283. V.T.Nguyen, L.Q.Ha, T.D.Nguyen, P.H.Ly, D.M.Nguyen, D.Hoang. *ACS Omega*, **7**, 1003 (2021)
284. L.Mo, S.Zhang, F.Qi, A.Huang. *Int. J. Biol. Macromol.*, **209**, 1922 (2022)
285. Y.Kim, J.Park, J.Bang, J.Kim, H.-J.Jin, H.W.Kwak. *J. Hazardous Mater.*, **426**, 128078 (2022)
286. V.Sharma, T.Shahnaz, S.Subbiah, S.Narayanasamy. *J. Polym. Environment.*, **28**, 2008 (2020)
287. E.M.Ahmed. *J. Adv. Res.*, **6**, 105 (2015)
288. E.E.Ureña-Benavides, G.Ao, V.A.Davis, C.L.Kitchens. *Macromolecules*, **44**, 8990 (2011)
289. K.J.De France, T.Hoare, E.D.Cranston. *Chem. Mater.*, **29**, 4609 (2017)
290. C.Xu, B.Z.Molino, X.Wang, F.Cheng, W.Xu, P.Molino, M.Bacher, D.Su, T.Rosenau, S.Willför. *J. Mater. Chem. B*, **6**, 7066 (2018)
291. R.M.Barajas-Ledesma, L.Hossain, V.N.Wong, A.F.Patti, G.Garnier. *J. Colloid Interface Sci.*, **599**, 140 (2021)
292. X.Xu, X.-k.Ouyang, L.-Y.Yang. *J. Mol. Liquids*, **322**, 114523 (2021)
293. C.R.Bauli, G.F.Lima, A.G.de Souza, R.R.Ferreira, D.S.Rosa. *Colloids Surfaces A: Physicochem. Eng. Aspects*, **623**, 126771 (2021)
294. H.l.Thérien-Aubin, Y.Wang, K.Nothdurft, E.Prince, S.Cho, E.Kumacheva. *Biomacromolecules*, **17**, 3244 (2016)
295. N.Masruchin, B.-D.Park, V.Causin. *Cellulose*, **25**, 485 (2018)
296. C.Siangsanoh, S.Ummartyotin, K.Sathirakul, P.Rojanapanthu, W.Treesuppharat. *J. Mol. Liquids*, **256**, 90 (2018)
297. A.E.Way, L.Hsu, K.Shanmuganathan, C.Weder, S.J.Rowan. *ACS Macro Lett.*, **1**, 1001 (2012)
298. J.S.Gonzalez, L.N.Ludueña, A.Ponce, V.A.Alvarez. *Mater. Sci. Eng.: C*, **34**, 54 (2014)
299. F.N.M.Padzil, S.H.Lee, Z.M.A.a.Ainun, C.H.Lee, L.C.Abdullah. *Materials*, **13**, 1245 (2020)